UCRL-17619 and errata
cy. 2

# University of California

# Ernest O. Lawrence Radiation Laboratory

PRODUCTION OF K MESONS IN THREE-BODY STATES IN PROTON-PROTON INTERACTIONS AT 6 BeV/c

W. Chinowsky, R. R. Kinsey, S. L. Klein,
M. Mandelkern, J. Schultz, F. Martin,
M. L. Perl, and T. H. Tan

August 29, 1967

TWO-WEEK LOAN COPY

This is a Library Circulating Copy which may be borrowed for two weeks. For a personal retention copy, call Tech. Info. Division, Ext. 5545

UCRL - 17619 cy. 2

## DISCLAIMER

This document was prepared as an account of work sponsored by the United States Government. While this document is believed to contain correct information, neither the United States Government nor any agency thereof, nor the Regents of the University of California, nor any of their employees, makes any warranty, express or implied, or assumes any legal responsibility for the accuracy, completeness, or usefulness of any information, apparatus, product, or process disclosed, or represents that its use would not infringe privately owned rights. Reference herein to any specific commercial product, process, or service by its trade name, trademark, manufacturer, or otherwise, does not necessarily constitute or imply its endorsement, recommendation, or favoring by the United States Government or any agency thereof, or the Regents of the University of California. The views and opinions of authors expressed herein do not necessarily state or reflect those of the United States Government or any agency thereof or the Regents of the University of California.

To be submitted to Physical Review

UCRL-17619
Preprint

UNIVERSITY OF CALIFORNIA

Lawrence Radiation Laboratory
Berkeley, California

AEC Contract No. W-7405-eng-48

# PRODUCTION OF K MESONS IN THREE-BODY STATES IN PROTON-PROTON INTERACTIONS AT 6 BeV/c

W. Chinowsky, R. R. Kinsey, S. L. Klein,
M. Mandelkern, J. Schultz, F. Martin,
M. L. Perl, and T. H. Tan

August 29, 1967

November 1967

TO: Recipients of UCRL-17619

FROM: Tech. Info. Div., IRL Berkeley

ERRATA

PRODUCTION OF K MESONS IN THREE-BODY STATES IN PROTON-PROTON INTERACTIONS AT 6 BeV/c

W. Chinowsky, R. R. Kinsey, S. L. Klein, M. Mandelkern, and J. Schultz[+]

Lawrence Radiation Laboratory, University of California, Berkeley, California

and

F. Martin, M. L. Perl, and T. H. Tan

Stanford Linear Accelerator Center, Stanford University, Stanford, California

Page 1 Lines 6-9. Cross sections should have the units μb.

Page 2 Line 8 should read "....belongs to a $\overline{10}$ representation.."

Page 3 The 7th line from bottom should read "The optical elements determining the focal properties of the beam at the uranium collimator were the first quadrupole pair, which yielded...."

Page 7 Line 18 should read "we impose a minimum projected decay angle...."

Page 9 Line 10 should read "....limits on $YK^+$ effective mass ...."

Page 13 The formula at the bottom should read "$F(M^2, \Delta^2) = \ldots.$"

Page 15 The 5th line from the bottom should read "to a single $F_{5/2}$ resonance...." The last line should read "Use of a $D_{5/2}$ resonance gives an equivalently good fit with comparable fraction of resonance production."

Page 17 Formulas after line 4 should read

$$\frac{d^4\sigma}{dM^2 d\Delta^2 d\Omega} = \frac{1}{4\pi}\frac{G^2}{4\pi}\frac{1}{(2\bar{p}\,\bar{E})^2}\frac{\Delta^2 + (m_p - m')^2}{(\Delta^2 + \mu^2)^2}\, kM\,\frac{d\sigma(M)}{d\Omega}$$

$$k = \frac{1}{M}\left[\frac{M^4}{4} - \frac{M^2}{2}(m_p^{\,2} + \mu^2) - \frac{1}{4}(m_p^{\,2} - \mu^2)^2\right]^{1/2}$$

Page 18 The 4th line from bottom should read "(d) are, respectively, $5.0(\mathrm{BeV}/c^2)^2$ and $1.8(\mathrm{BeV}/c^2)^2$."

Page 18 The 3rd line should read "In Figs. 18a and 18b we show the predictions of each model for the distribution in $\Delta^2$, the momentum transfer to the recoil baryon, for reactions (a) and (d) respectively"

Page 20 The first line should read "angular distributions of the $\Sigma^+$ and $\Lambda$ in the...."

Page 23 Line 17 should read "J. D. Jackson, J. T. Donahue, K. Gottfried, R. Keyser , and B. E. Y. Svensson, Phys. Rev. 139B, 428 (1965)."

Page 28 The 3rd line should read "makes with the beam proton in the overall center of mass, light line: only unambiguously identified examples of the reaction $pp \rightarrow \Lambda pK^+$ and $pp \rightarrow \Sigma^0 pK^+$."

Page 29 Line 10 should read "$pp \rightarrow \Lambda K^+ p$."

November 1967

TO: Recipients of UCRL-17619

FROM: Tech. Info. Div., IRL Berkeley

ERRATA

PRODUCTION OF K MESONS IN THREE-BODY STATES IN PROTON-PROTON INTERACTIONS AT 6 BeV/c

W. Chinowsky, R. R. Kinsey, S. L. Klein, M. Mandelkern, and J. Schultz[+]

Lawrence Radiation Laboratory, University of California, Berkeley, California

and

F. Martin, M. L. Perl, and T. H. Tan

Stanford Linear Accelerator Center, Stanford University, Stanford, California

Page 1 Lines 6-9. Cross sections should have the units μb.

Page 2 Line 8 should read "....belongs to a $\overline{10}$ representation.."

Page 3 The 7th line from bottom should read "The optical elements determining the focal properties of the beam at the uranium collimator were the first quadrupole pair, which yielded...."

Page 7 Line 18 should read "we impose a minimum projected decay angle...."

Page 9 Line 10 should read "....limits on $YK^+$ effective mass ...."

Page 13 The formula at the bottom should read "$F(M^2, \Delta^2) = \ldots$."

Page 15 The 5th line from the bottom should read "to a single $F_{5/2}$ resonance...." The last line should read "Use of a $D_{5/2}$ resonance gives an equivalently good fit with comparable fraction of resonance production."

Page 17 Formulas after line 4 should read

$$\frac{d^4\sigma}{dM^2 d\Delta^2 d\Omega} = \frac{1}{4\pi}\frac{G^2}{4\pi}\frac{1}{(2\bar{p}\,\bar{E})^2}\frac{\Delta^2 + (m_p - m')^2}{(\Delta^2 + \mu^2)^2}\, kM\,\frac{d\sigma(M)}{d\Omega}$$

$$k = \frac{1}{M}\left[\frac{M^4}{4} - \frac{M^2}{2}(m_p^{\,2} + \mu^2) - \frac{1}{4}(m_p^{\,2} - \mu^2)^2\right]^{1/2}$$

Page 18 The 4th line from bottom should read "(d) are, respectively, $5.0(\mathrm{BeV}/c^2)^2$ and $1.8(\mathrm{BeV}/c^2)^2$."

Page 18 The 3rd line should read "In Figs. 18a and 18b we show the predictions of each model for the distribution in $\Delta^2$, the momentum transfer to the recoil baryon, for reactions (a) and (d) respectively"

Page 20 The first line should read "angular distributions of the $\Sigma^+$ and $\Lambda$ in the...."

Page 23 Line 17 should read "J. D. Jackson, J. T. Donahue, K. Gottfried, R. Keyser , and B. E. Y. Svensson, Phys. Rev. 139B, 428 (1965)."

Page 28 The 3rd line should read "makes with the beam proton in the overall center of mass, light line: only unambiguously identified examples of the reaction $pp \rightarrow \Lambda pK^+$ and $pp \rightarrow \Sigma^0 pK^+$."

Page 29 Line 10 should read "$pp \rightarrow \Lambda K^+ p$."

# PRODUCTION OF K MESONS IN THREE-BODY STATES IN PROTON-PROTON INTERACTIONS AT 6 BeV/c*

W. Chinowsky, R. R. Kinsey, S. L. Klein, M. Mandelkern, and J. Schultz+

Lawrence Radiation Laboratory, University of California, Berkeley, California

and

F. Martin, M. L. Perl, and T. H. Tan

Stanford Linear Accelerator Center, Stanford University, Stanford, California

August 29, 1967

ABSTRACT

Analysis of 9700 events, containing at least one observed neutral or charged decay, produced by 6 BeV/c protons in the LRL 72" liquid hydrogen bubble chamber has yielded 1746 examples of the reaction proton + proton → hyperon + K meson + nucleon. Productions cross sections for these three body reactions are

$$\sigma(\Lambda K^+p) = 54 \begin{smallmatrix} +3 \\ -5 \end{smallmatrix}$$

$$\sigma(\Sigma^0 K^+p) = 17 \begin{smallmatrix} +4 \\ -2 \end{smallmatrix}$$

$$\sigma(\Sigma^+ K^0 p) = 26 \pm 4$$

$$\sigma(\Sigma^+ K^+ n) = 57 \pm 7$$

Strong $N^*$ production is observed in all channels. In particular one or more T=1/2 resonant states with mass near 1700 MeV/$c^2$, decaying into $\Lambda K^+$, and a T=3/2 resonance with mass 1920 MeV/$c^2$, decaying into $\Sigma^+K^+$ are produced. In all cases the data are consistent with a production process dominated by a single pion exchange mechanism. No evidence is found for a dibaryon state in either the Λ-proton or Σ-nucleon system.

---

* Work done under the auspices of the U.S. Atomic Energy Commission.

+ Present address: University of California, Irvine, California

## I. INTRODUCTION

It has been well established that the strong interactions of mesons with nucleons, and of mesons with mesons, are invariant to a good approximation under the operations of the group SU(3). As first discussed by Oakes,[1] it is straightforward to extend the application of this symmetry requirement to the baryon-baryon interaction and in particular to classify multi-baryon states as members of irreducible representations of this group. Since the nucleon is a member of an octet it follows that the deuteron, a system of hypercharge two and isotopic spin zero, belongs to a 10 representation and the virtual isotopic triplet state of the deuteron occurs in a 27 representation. The validity of this classification and thus of the relevance of SU(3) symmetry to the nuclear-binding interactions would be most directly established by the discovery of other members of the representations as bound states or resonant interactions of hyperon and nucleon or hyperon and hyperon. Investigations of hyperon-nucleon interactions, both in elastic scattering[2] and final-state interactions[3] of particles produced in nucleon-nucleon collisions have not as yet yielded any conclusive evidence for a resonance in the hyperon-nucleon system. The only indication of such a resonance is the reported enhancement in the Λ-p mass spectrum near minimum Λ-p mass in small momentum transfer p-p collisions.[3] To search more intensively for such baryon-baryon states and to reveal more general details of nucleon-nucleon reaction mechanisms, an extensive study of proton interactions in the LRL 72" liquid hydrogen bubble chamber was undertaken. We report here results on the observed characteristics of hyperon production in three-body final states via the

channels

$$pp \rightarrow \Lambda K^{+}p \quad .... \quad (a)$$
$$\Sigma^{o}K^{+}p \quad .... \quad (b)$$
$$\Sigma^{+}K^{o}p \quad .... \quad (c)$$
$$\Sigma^{+}K^{+}n \quad .... \quad (d)$$

The states produced in these reactions would appear to be most suitable for elucidation of final-state hyperon-nucleon interactions, whose effects might be obscured in states including pions by the presence of $Y^{*}$, $N^{*}$, and $K^{*}$ resonances. The data reported result from analysis of approximately 500,000 photographs, taken in two separate running periods, of interactions of protons in a beam averaging ten particles per pulse. The incident momentum was 6.10 ± .02 BeV/c during the first running period and 6.00 ± .02 during the second.

## II. EXPERIMENTAL PROCEDURE

Protons produced in a target 3/8" high, 1/4" transverse to and 1/2" along the direction of the external proton beam of the Bevatron were transported to the bubble chamber using the arrangement shown schematically in Fig. 1. The optical elements determining the focal properties of the beam at the slit S2 were the quadrupole pair Q1Q2, which yielded vertical magnification 0.5 and unit horizontal magnification, and the two bending magnets producing a dispersion of one inch per 1% $\Delta P/P$. Momentum definition of ±0.15% was provided by the slit, of dimensions 1/2" vertically and 1/4" horizontally, in the 12" thick uranium collimator. To allow multiple operation of external beam foci, targeting techniques were needed which

would minimize interference with external beam optics since the target could not conveniently be located at an image position. In the first running period, during which about half the photographs were taken, a polyethylene target was fixed in position in the beam. During the remainder of the run a copper target was fixed at a distance of 3/4" from the normal external beam position and the beam deflected on to it by a magnet[4] pulsed on for approximately 200 μsec. In this way, independent intensity control was achieved with the remainder of the beam available for other experiments. Beam intensity required was $\sim 10^{11}$ protons/pulse for the first targeting arrangement and $\sim 5 \times 10^{10}$ protons/pulse for the second. Increased efficiency of operation was achieved with dynamic intensity control provided by a pulsed parallel plate electromagnetic separator operated with a 4" gap and 150 kilovolts between the plates.[5] An appropriate signal from a preset scalar reading the output of counters directly before the entrance window of the bubble chamber triggered a spark gap across the spectrometer plates which discharged them in 2 μsec. The magnetic field remained and caused the beam to be deflected 3/4" vertically, off slit S2 into the uranium collimator. In this way the usual variations in beam intensity due to statistical fluctuations and accelerator instability were largely eliminated. With a total beam in the channel of about 30 particles per pulse, the beam at the chamber was maintained constant to within two tracks per picture. Contamination from single pion production in the target was small since the primary proton beam and the secondary protons from the target were set to differ little in momentum, while the secondary pions had considerably lower momentum. A measurement made in a similar beam[6]

using a Cerenkov counter to distinguish pions from protons indicated a pion contamination of less than 0.1%. This was neglected as a source of background events in the analysis.

All the film has been scanned twice for events of interest. All events containing one or more charged or neutral decays were recorded and measured with conventional digitized measuring machines. Geometrical reconstruction and kinematical fitting of events with neutral V's was done with the use of the program PACKAGE. Of the three views measured only the two chosen by the program to give maximum accuracy in determination of the dip angle of each track were used. Reconstruction and fitting of two-prongs with charged decays was done with TVGP-SQUAW which uses measurements in three views for reconstruction. The incident beam momentum was determined from measurements of non-interacting tracks and from well-identified examples of fits to elastic scattering. Both methods gave the same result. The observed width of the beam momentum distribution was consistent with that expected only from measurement error, approximately 1%. However, we assign ±0.5% uncertainty to the incident particle momentum for fitting purposes, allowing a rather larger spread than deduced from beam optics for effects such as scattering on slits and windows.

A total of 7200 events of two-prongs and one neutral V, and 2500 of two prongs with the decay of either or both outgoing charged particles, candidates for events containing three final-state particles, were measured. Identity of the outgoing particles was established by the usual methods of requiring consistency of measured momenta with reaction kinematics and visually estimated bubble densities. The $\chi^2$ for the kinematic fit was required to correspond

to a probability level greater than 1%. In this way 1302 events with neutral V's were identified as examples of three-body channels a, b, and c. Of these events, 45 were also consistent with four-body final states. They were assigned to the three body category because the three-body fits are more constrained by the kinematical requirements. Similarly all the ambiguities between $\Sigma^{o}pK^{+}$ and $\Lambda pK^{+}$ were resolved in favor of the $\Lambda$ since the fit with a $\Lambda$ has four constraints and that with a $\Sigma^{o}$ only two. The decision in this case is greatly strengthened by appeal to the requirement that the angular distribution of any particle with respect to the incident beam direction be symmetrical about $90^{o}$ in the center-of-mass system. In Fig. 2 we show the angular distribution of the proton produced with a hyperon and $K^{+}$ for the weighted total of 533 events with uniquely identified $\Lambda$'s , together with that including the 504 events with ambiguous identification of the hyperon. Clearly the symmetry is improved if the events are combined. Thus, in all such cases of ambiguity the hyperon is considered to be a $\Lambda$. The angular distribution of the protons produced in unambiguous examples of the $\Sigma^{o}pK^{+}$ final state is shown in Fig. 3. This distribution is not nearly as symmetric as that for $\Lambda pK^{+}$ reflecting the greater difficulty in resolving ambiguities with the two constraint fit. The asymmetry is, however, in the same direction as that of the ambiguities which were assigned to $\Lambda pK^{+}$ and thus does not result from inclusion of misidentified $\Lambda$ production events. We conclude that the source of this asymmetry is ambiguity with four-body hypotheses which have one constraint, and that the four-body background plus events lost due to misidentification amounts to about 10% of the sample, judging from the number of ambiguous events and the size

of the production asymmetry.

Since the reaction (d) always yields an unobserved neutral product, kinematical constraints may be applied only if the $\Sigma^+$ momentum is known from measurement of the $\Sigma^+$ track and/or measurement of the decay product track. In either event, the momentum is generally poorly determined and kinematical ambiguities are more serious. Three kinds of ambiguities were present: those involved in (i) distinguishing between $\Sigma^+$ decays and $K^+$ decays, (ii) distinguishing $\Sigma^+nK^+$ from $\Sigma^+pK^o$ with unobserved $K^o$ decay, and (iii) separating events with an additional, unobserved neutral. In fact only an insignificant number of the first and second kinds appear, fitting to the decay kinematics and bubble density estimates generally being sufficient to distinguish among the various hypotheses. Further, the ratio of observed numbers of $\Sigma^+pK^o$ with $K^o$ decay to the number with unobserved $K^o$ decay, after correction for detection inefficiency and scanning biases, is $.9 \pm 0.3$, indicating that the correct number of identifications of $\Sigma^+pK^o$ events has been made. In the analysis of reaction (d) only the events consistent with $\Sigma^+ \rightarrow n\pi^+$ were used. This procedure is required since, to correct for scanning inefficiency, we impose a minimum laboratory decay angle cut-off of $10^o$. The decay angle of the proton from a $\Sigma^+$ with momentum greater than 1.4 BeV/c is necessarily smaller than $10^o$. We find that the corrected sample of data for reaction (d) is consistent with symmetry in the total center-of-mass frame and estimate from the number of ambiguities that contamination is $5 \pm 2\%$.

In these ways, ambiguities in identification were settled and events were assigned to particular categories. Table I gives the total number of observed events for each of the four reactions.

## III. PRODUCTION CROSS SECTIONS

Some fraction of events produced in the chamber escape detection in both scans. Corrections to the observed body of data, in addition to that due to ordinary scanning inefficiency, must then be made for inefficient detection of decays at small angles, decays at small and large distances from the production origin, as well as for undetected decays into neutral particles. Examination of the observed distributions of decays in time and angle permit estimates to be made of the detection efficiency. In addition the requirement of a symmetric production angular distribution aids in determining detection biases. To correct for these inefficiencies, each event was weighted by the inverse of the probability for detection within the kinematic region determined by requiring events to be within a fiducial volume, to have decays with projected opening angles greater than $10^{\circ}$ and less than $75^{\circ}$ and lengths greater than minima determined by particle identification: 1.5 cm for $\Lambda$'s and $K^{0}$'s, 1.0 cm for $\Sigma^{+}$'s. The magnitude of these corrections may be inferred from the corrected numbers of events listed in Table I. The incident flux needed to compute the cross sections quoted in Table I was determined from a count of beam tracks in frames selected at regular intervals throughout the film. The scanning-measuring efficiencies were deduced from a comparison of processed events from the two scans and were found to be 80 ± 3% for scan I, 81 ± 3% for scan II. Errors quoted include statistical error in the number of events, an estimate of ±3% error in flux determination, and estimated error ±5% resulting from misidentifications and uncertainties in the magnitudes of the various corrections.

## IV. ANALYSIS OF FINAL STATE INTERACTIONS

The four states studied, $\Lambda pK^+$, $\Sigma^o pK^+$, $\Sigma^+ pK^o$, and $\Sigma^+ K^+ n$ have similar properties in many respects. We will discuss them simultaneously as much as possible. Figures 4, 5, 6, 7 are scatter plots of the squares of the effective masses of hyperon-nucleon vs hyperon-kaon systems. In each case a non-uniform density within the kinematic boundary of the Dalitz plot is apparent. A strong concentration of data points is noted at low values of Y-K mass, particularly in the $\Lambda K^+$ and $\Sigma^+ K^+$ systems. In no case is there a clearly defined region in hyperon-nucleon effective mass within which the density of points is strikingly larger than in others. Rather, only in a region defined by limits on $\Lambda K^+$ effective mass is there such a concentration. The existence of only $\Lambda K^+$ and $\Sigma^+ K^+$ final-state interaction is demonstrated more conclusively in the effective mass distributions of Figs. 8, 9, 10, and 11 shown together with the corresponding phase space distributions. Corrections to the data have been made here for observational biases, so that each observed event is weighted as discussed above. The bin heights in each histogram are the sums of the weights for individual events falling into the relevant bins. Statistical errors are given by the application of Poisson statistics to a weighted collection of events, thus if

$$N = \sum_j w_j \quad , (\delta N)^2 = \sum_j w_j^{\,2} \quad .$$

The weights for reactions (a), (b), and (c) are relatively constant with average values 1.3, 1.3 and 1.6 respectively. The weights for reaction (d) are distributed over a broad range with average value 2.6; consequently, error bars are displayed on the histograms of Figs. 11 and 20.

In fact, none of the conclusions are substantially altered when unweighted distributions are considered. This is the case because only about 10% of the expected number of events with neutral V's, and 30% of the numbers with charged decays, are actually missing from the sample. In addition the detection inefficiencies are not strongly dependent on the momentum and angular distributions.

All the Y-N and Y-K mass distributions show considerable deviations from the statistical distribution but most of the further discussion will be limited to the $\Lambda pK^+$ and $\Sigma^+ nK^+$ states for a number of reasons. In the first state the hyperon-kaon system occurs only with isotopic spin T=1/2 and in the latter only with T=3/2, so that the analysis of resonance production is simplified. The $\Sigma^o pK^+$ and $\Sigma^+ pK^o$ reactions appear qualitatively to have properties similar to those discussed below and the samples of these are severely limited statistically and probably more contaminated. Analysis of the latter reactions does not add to the conclusions about final-state interactions nor to the further elucidation of the production dynamics.

We have noted the non-uniformity in the Dalitz plot and the corresponding enhancements at low hyperon-kaon mass and high hyperon-nucleon mass. While it is not possible, in general, to demonstrate rigorously which of the two-body combinations are in resonance, we can nevertheless argue persuasively that the details of the non-uniformity are consistent with the production of only Y-K resonances. A simple check of this hypothesis consists of alternately assuming production of the Y-K and Y-N systems with the observed mass distributions, followed by isotropic decay in their center-of-mass frames, and calculating the expected reflections in the

Y-N and Y-K systems, respectively. The results of such calculations are shown in Fig. 8 for the $\Lambda pK^+$ reaction. It is clear that the $\Lambda p$ peak can be understood as a reflection of a $\Lambda K^+$ enhancement, while the converse does not hold.

The above assumption of an isotropic disintegration of the two-body system cannot be completely justified. The break-up angular distributions of either two-body system can be readily obtained from the Dalitz plots, Fig. 4-7. The abscissa and ordinate may be interpreted respectively as the square of the Y-K mass and the cosine of the angle between the nucleon and the Y-K line of flight in the Y-K center-of-mass system. The latter angle need not be isotropically distributed, as a consequence of the production mechanism, or final-state interactions. A new hyperon-nucleon resonance with a pathologically anisotropic decay distribution could be invoked to explain the overall distribution in the Dalitz plot and the Y-K enhancement as a reflection. It is quite unnecessary to invoke such a new resonance with complicated properties, but we rather attribute the distribution purely to already well-established Y-K resonant interactions, specifically $N^*_{1/2}(1688)$ and $N^*_{3/2}(1920)$.

This conclusion is greatly reinforced by the observation that the Y-K production is predominantly peripheral and consistent with a single pion exchange model as discussed below. It should be noted that if those events produced with low momentum transfer to the inital proton are eliminated from the $\Lambda p$ mass distribution, a spectrum results that is in excellent agreement with phase space, as seen in Fig. 12. Thus, even in the region where peripheralism does not dominate, there is no suggestion of

a dibaryon resonance. In calculating momentum transfer, there are of course two values for each event since the initial state protons are indistinguishable. We use the smaller momentum transfer to define the identities of the initial state protons when comparing with dynamical models and require our theoretical calculations to be consistent with this procedure. Such a choice is suggested by the strong peaks at low momentum transfer, which characterize peripheral production. This procedure is well justified by the further demonstration below that the mechanism is indeed peripheral.

The $\Lambda p$ and $\Lambda K^+$ mass spectra may be understood to result from a quasi-two-body process, $pp \rightarrow N^*_{1/2}p$ , proceeding via a peripheral mechanism, with subsequent decay of the $N^*$ into $\Lambda K^+$. The conclusion that there is no evidence for a $\Lambda p$ resonant state in in agreement with that of Bierman, et al.[7] The $K^+p$ mass distribution for this reaction, Fig. 8c, shows structure not observed in $K^+p$ elastic scattering with enhancements at 1.8 and 2.1 BeV/$c^2$. Thses features cannot be directly explained as reflections of the $N^*_{1/2}(1688)$ production. However their absence in $K^+p$ elastic scattering suggest that the peaks observed here are not resonances, but rather kinematical correlations associated with other aspects of the production process.

Consequently we conclude that we have observed no dibaryon resonances in either the T=1/2 or the T=3/2 in the mass range from 2.05 to 3.14 BeV/$c^2$. It is conceivable that a dibaryon resonance in this range would be difficult to detect above the background of peripherally prodeuced events in this reaction. Nevertheless the absence of distinct

localized enhancements in the hyperon-nucleon mass spectrum leads to the above conclusion. Further, we estimate that the cross section for the production of the enhancement reported by Melissinos et al.[3] is less than 0.2 μb in the present experiment.

## V. NUCLEON ISOBAR PRODUCTION

Analyses of pion nucleon elastic scattering have revealed evidence for the existence of three T=1/2 resonances near 1690 MeV and one T=3/2 resonance near 1920 MeV total c.m. energy.[8] The properties of these resonances inferred from the phase shift analyses are listed in Table II. We interpret the observed resonance production as production of these pi-nucleon resonances and their subsequent decay into hyperon and kaon.

Analysis of the angular and polarization distributions observed in $\pi^+ p \rightarrow \Sigma^+ K^+$ [9] show that this reaction proceeds in part through an $F_{7/2}$ resonance at 1925 MeV with width Γ=175 MeV, consistent with the parameters of the resonance observed in pi-nucleon elastic scattering. The partial width of the $F_{7/2}$ into $\Sigma^+ K^+$ was found to be about 1 MeV. Our peak in the $\Sigma^+ K^+$ mass spectrum in the channel $\Sigma^+ n K^+$ is naturally interpreted as due to the production of this resonance and its subsequent decay into $\Sigma^+ K^+$. To estimate the rate of resonance production the distribution in $\Delta^2$, momentum transfer to the neutron, and M, $\Sigma^+ K^+$ effective mass, was fitted to the expression

$$F(M,\Delta^2) = \frac{1}{(\alpha+\Delta^2)^2} \frac{q}{M} \left[ 1 + c \frac{\Gamma_{\Sigma^+K^+}(M)}{(M_o^2 - M^2)^2 + M_o^2 \Gamma^2} \frac{M^2}{q} \right] \qquad (1)$$

which is a sum of resonance and background contributions. The form factor

$1/(\alpha+\Delta^2)^2$ is required to parameterize the strong peripheralism shown in the data. Here q is the momentum of the $\Sigma^+$ in the $\Sigma^+K^+$ rest frame, $M_o$ the resonance energy quoted in Table II, $\Gamma$ the total width and c a number which characterizes the production cross section. The energy dependent partial width into the channel $\Sigma^+ + K^+$ can be taken to be

$$\Gamma_{\Sigma^+K^+} = \Gamma^o_{\Sigma^+K^+} \frac{(q/q_o)^{2\ell+1}(M_o/M)}{(q^2+X^2)^\ell/(q_o{}^2+X^2)^\ell} \qquad (2)$$

The "partial width" $\Gamma^o_{\Sigma^+K^+}$ is a measure of the coupling of the resonance to the decay channel in question and the rest of the expression is the product of phase space, a barrier penetration factor, and form factor normalized to unity at the central mass $M_o$ of the resonance. Both these latter factors depend strongly on the orbital angular momentum $\ell$ of the decay products. The X in the form factor is essentially the inverse of an effective range of interaction.[10]

The total width can be taken to be the sum of the energy dependent partial widths for all decay modes. In principle it is possible to determine both c and $\Gamma^o_{\Sigma^+K^+}$ by fitting. However since the $\Sigma^+K^+$ partial width is very small compared to the total width, the shape of the distribution is insensitive to the partial width and only the product $c\Gamma^o_{\Sigma^+K^+}$ is determined. We take the total width to be that obtained from pi-nucleon scattering data and $c\Gamma^o_{\Sigma^+K^+}$ then determines the percentage of resonance production in this reaction. We find 38 ± 5% of the events result from resonance production and 62 ± 5% from background. The parameter $\alpha$ is found to be .35 ± .05 $(\mathrm{BeV}/c)^2$.

Determination of the rate of resonance production in the $\Lambda pK^+$ channel is rather more complicated. As mentioned above, there are three $\pi p$ resonances near 1690 MeV. None of the branching ratios for decay into $\Lambda K^+$ is firmly known, nor have the relative production rates of these resonances been measured from non-strange particle production in p-p collisions. Some information about the parameters of these resonances has been obtained however from analysis of the differential cross section and $\Lambda$ polarization in $\Lambda K^0$ production in $\pi^- p$ collisions.[11] Reasonable agreement results with a J=5/2 resonance with parity either positive or negative, total width ~ 100 MeV and partial width into $\Lambda K^0$ ~ 1-10 MeV. No analysis finds any evidence for the S-wave resonance in the $\Lambda K^0$ system. Appeal to the requirements of $SU_3$ symmetry to determine branching ratios of the $5/2^+$ and $5/2^-$ $N^*$'s are useless since both resonances are thought to be members of octets and their partial widths are sensitive functions of their D/F ratios. For example, a D/F ratio of 3 forbids decay into $\Lambda K$. The study of baryon resonances[12] suggests that this ratio is often widely different in different $N^*$ octets.

The data from this experiment are insufficient to determine the contributions of the various resonances. Since the associated production data suggest a large J=5/2 amplitude we fit the $\Lambda K^+$ mass spectrum to a single J=5/2 resonance at 1688 MeV together with a background contribution. As in the $\Sigma^+ nK^+$ case, we fit to an expression corresponding to (1) and find 54 ± 6% of the events result from resonance production and 46 ± 6% from background. The fitted value for $\alpha$ is .53 ± .03$(\mathrm{BeV/c})^2$. Use of a $D_{5/2^+}$ resonance gives equivalent results.

In principle the angular distribution of the resonance decay products can provide the necessary information to determine the spin and parity of the parent state. In Fig. 13 we show the angular distribution, with respect to the momentum transfer direction, of the hyperon in the $\Sigma^+K^+$ c.m. system and in Fig. 14 that for the $\Lambda K^+$. Predictions of a $\pi$ exchange model for production shown here with the experimental distributions will be discussed below. In both reactions the data in the resonance region are consistent with a resonance decay symmetric about $90^\circ$ superimposed on a small amount of asymmetric background. The spin density matrix of the resonance is not simply determined in proton-proton interactions, even for forward production. The possible angular distributions for high spin resonances are rather complex and with the limited statistical accuracy of the data it is not possible to identify the contributing states.

## VI. ONE MESON EXCHANGE MECHANISMS

As noted above the production angular distributions show the characteristic feature of peripheralism, a strong correlation between the final and initial state baryon directions. We display in Figs. 15 and 16 scatter plots of hyperon-kaon mass versus momentum transfer to the final state nucleon, showing the high concentration of events at small momentum transfers. To determine the compatibility of the data with predictions of simple models for peripheral production; in particular one particle exchange processes, detailed comparisons have been made for the reactions $pp \rightarrow \Sigma^+K^+n$ and $pp \rightarrow \Lambda K^+p$.

It is clear that of the three lowest order diagrams shown in Fig. 17, only the meson exchange processes, 17a, 17b, yield the observed characteristics. Calculations were made for the pion and kaon exchange models, using a Monte Carlo method to generate events distributed according to:[13,14]

$$\frac{d^4\sigma}{dM^2 d\Delta^2 d\Omega} = \frac{1}{4\pi}\,\frac{G^2}{4\pi}\,\frac{1}{(2\bar{p}\,\bar{E})^2}\,\frac{\Delta^2+(m_p{}^2-m'^2)}{(\Delta^2+\mu^2)^2}\,k\,M\,\frac{d\sigma(M)}{d\Omega} \qquad (3)$$

where

$$k = \frac{1}{M}\,\frac{M^4}{4} - \frac{1}{2}M^2(m_p{}^2+\mu^2) + \frac{1}{4}(m_p{}^2-\mu^2)^{1/2}$$

$\bar{p}$, $\bar{E}$ are the center-of-mass momentum and energy of the incident proton;

$\frac{G^2}{4\pi}$ = meson baryon-baryon coupling constant describing vertex A in Fig. 19;

we use $\frac{G^2_{pp\pi^o}}{4\pi} = 15$, $\frac{G^2_{p\Lambda K^+}}{4\pi} = 15$ ; $\frac{G^2_{p\Sigma^+K^o}}{4\pi} = .64$

$\Delta^2$ = four momentum transfer squared to the recoil baryon m'; a nucleon for $\pi$ exchange, $\Lambda$ or $\Sigma$ for K exchange;

$\mu$ = mass of exchanged meson, $m_p$ = mass of proton;

M = invariant mass of the particles emerging at vertex B , e.g., $\Lambda K^+$ or $\Sigma^+K^+$ for $\pi$ exchange;

$\frac{d\sigma(M)}{d\Omega}$ is the differential cross section for the two-body production at vertex B,[15] $\pi p \rightarrow YK$ or K nucleon elastic or charge exchange scattering;

k is a kinematic factor which can be identified as the 3-momentum of the exchanged meson in the YK or NK center-of-mass frame consistent with actual two-body scattering at energy M.

The Monte Carlo technique provides great flexibility in the comparison of the theory with experiment. Any procedure applied to the actual data can be used on the events generated by the Monte Carlo program. Thus we

include the effect of selecting the smaller value of momentum transfer to define the event and any other relevant kinematic selections applied to the experimental distributions. In Fig. 18 we show the predictions of each model for the distribution in $\Delta^2$, the momentum transfer to the recoil baryon. It is clear that in each case the experimental peak at small values is considerably narrower than that predicted. This feature of stronger damping at large momentum transfer has been demonstrated often in many peripheral processes.[14] Most other features of the data are reasonably consistent with a single meson exchange mechanism and the momentum transfer discrepancy may be attributed to corrections to the model. In particular, absorption effects[14] due to competing inelastic channels, vertex form factors,[13] and off-the-mass shell corrections are known to modify the $\Delta^2$ dependence given by the propagator and vertex term in the simple single-particle exchange process. Since the momentum transfer distribution implies kinematic restrictions on the values other variables may assume, we include in further calculations a form factor, $F(\Delta^2)$, multiplying the above expression (3). The functional form, chosen so that the modified expression reproduces the dependence of the data on $\Delta^2$ is

$$F(\Delta^2) = \left(\frac{A-M^2_{exch}}{A+\Delta^2}\right)^2 .$$

For the pion-exchange case the fitted values for A, in reactions (a) and (d) are, respectively, 5.0 BeV/$c^2$ ; 1.8 BeV/$c^2$.

The most striking feature in either channel considered is the hyperon-kaon mass spectrum which must of course be reproduced by a relevant model. Predictions of both K-exchange and $\pi$-exchange are shown

in Figs. 19 and 20. In both cases the $\pi$-exchange model satisfactorily reproduces the peaks in the $\Lambda K^+$ and $\Sigma^+K^+$ spectra while agreement with the K-exchange model is poor. The total cross sections calculated from the unmodified $\pi$-exchange mechanism are 96 $\mu$b and 414 $\mu$b for the $\Lambda pK^+$ and $\Sigma^+K^+n$ channels respectively while the unmodified K-exchange model gives 3.2 mb and 40 $\mu$b. Addition of the form factor reduces the $\pi$-exchange predictions to 60 $\mu$b and 130 $\mu$b and the K-exchange predictions to approximately 320 $\mu$b and 5 $\mu$b. There is considerable uncertainty in the K-exchange predictions due to the inadequacy of a one-parameter form factor of the above form in this case. Both the modified and unmodified $\pi$-exchange predictions are in better agreement with the experimental data than the corresponding K-exchange prediction. As a further test of the model, we examine the $\Lambda$ polarization obtained from the angular distribution of the decay products of the $\Lambda$ in its rest frame. The polarization is measured along the normal to the plane containing the directions of the $\Lambda$ and relevant initial proton in the $\Lambda K^+$ center-of-mass system. We show in Fig. 21 experimental values for the $\Lambda$ polarization averaged over intervals in $\Lambda K^+$ mass, together with the predictions of pion exchange. Considerable polarization is noted, particularly at low momentum transfer and low $\Lambda K^+$ mass, in agreement with the results obtained for the associated production reaction $\pi^- p \rightarrow \Lambda K^0$. The K-exchange model predicts zero polarization since only a p-wave $\Lambda$ production amplitude is present. Thus we find the data consistent with that expected for a dominant pion exchange mechanism with no evidence for a contribution from K exchange.

We now study the predictions of the $\pi$-exchange model in more

detail. Figures 13 and 14 show the angular distribution of the $\Lambda$ in the $\Lambda K^+$ center-of-mass system, with the momentum transfer as polar axis, together with the $\pi$-exchange predictions. Agreement is very satisfactory. In Figs. 22 and 23 we show the Treiman-Yang angle distributions and notice improved agreement with isotropy for events with small momentum transfer. Such substantially better agreement is to be expected in this region where the dominance of the pion exchange contribution over other mechanisms is enhanced. Some deviation from isotropy may be expected to result from misidentification of the initial state proton by selecting the lower momentum transfer. About seven percent of the events with $\Delta^2 \leq .5(\mathrm{BeV/c})^2$ are in fact produced with large $\Delta^2$, according to the distribution calculated with single pion exchange, and their inclusion results from misidentification. The "calculated" distributions include this non-isotropy since they come from a Monte Carlo calculation as discussed.

We conclude that the single pion-exchange mechanism with a form factor is in reasonable agreement with the data, particularly so at small momentum transfers. A more detailed analysis, involving absorbtive corrections is necessary to determine if the discrepancies such as the sharp momentum transfer peak and anisotropy in the Treiman-Yang angle distributions can be accommodated within a modified peripheral model. Unfortunately the complete lack of information about absorbtion in the final state makes such a calculation unfeasible.

## VII. CONCLUSIONS

Three-body strange particle states produced in proton-proton inter-

actions proceed dominantly through the pion exchange mechanism. There is considerable nucleon isobar production and these isobars, the $N^*_{3/2}(1920)$ and $N^*_{1/2}(1688)$ have properties consistent with those inferred from pion-nucleon scattering.

No evidence was found for the existence of a resonant hyperon-nucleon state with mass within the limits

$$2.05 \leq M_{\Lambda p} \leq 3.14 \text{ BeV}/c^2$$
$$2.15 \leq M_{\Sigma^+ n} \leq 3.14 \text{ BeV}/c^2 \quad .$$

## VIII. ACKNOWLEDGMENTS

Our particular thanks go to R. Watt and the bubble chamber crew for careful attention to operations during a long, arduous and sometimes excessively dull running period, with similar expressions of gratitude to the Bevatron operating crew.

We thank Professor L. Alvarez for making the bubble chamber available. Professor E. Segrè provided valuable support and encouragement continuously and we express our gratitude to him.

Mr. W. Gage, Mr. B. Douglass, and Miss M. Corey contributed invaluably to the programming efforts and the scanning and measuring personnel contributed with their usual skill and industry.

## REFERENCES


1. R. J. Oakes, Phys. Rev. 131, 2239 (1963).
2. B. Sechi-Zorn, R. A. Burnstein, T. B. Day, B. Kehoe, G. A. Snow, Phys. Rev. Letters 13, 282 (1964).

   L. Piekenbrock and F. Oppenheimer, Phys. Rev. Letters 12, 625 (1964).

   J. Schultz, R. Kinsey, W. Chinowsky, N. Rybicki, Bull. Am. Phys. Soc. Vol. 10 p. 529 (1965).

   R. Engelmann, H. Filthuth, V. Hepp, E. Kluge, Phys. Letters 21, 587 (1966).

   H. G. Dosch, R. Engelmann, H. Filthuth, V. Hepp, E. Kluge, Phys. Letters 21, 236 (1966).

   R. A. Burnstein, Univ. of Maryland Tech. Report No. 469 (1965).
3. A. C. Melissinos, N. W. Reay, J. T. Reed, T. Yamanouchi, E. Sacharidis, S. J. Lindenbaum, S. Ozaki, L. C. L. Yuan, Phys. Rev. Letters 14, 604 (1965).

   P. A. Piroùe, Phys. Letters 11, 164 (1964).

   W. J. Hogan, P. F. Kuny, A. Lemonick, P. A. Piroué, A. J. S. Smith, Bull. of the Am. Phys. Soc., Wash. Meeting p. 517 (1965).

   W. A. Wenzel, private communication.

   G. Alexander, O. Benary, B. Reuter, A. Shapiro, E. Simopoulou, G. Yekutieli, Phys. Rev. Letters 15, 207 (1965).
4. C. Dols, UCRL-8346, a quarterly report.
5. UCRL Engineering Note EET-1071. This method of beam control was suggested by J. Murray. The pulsing gear was constructed under the supervision of R. Force. We are indebted to them for the success of the operation.

6. We thank W. Wenzel for the use of equipment and aid in making this measurement.

7. E. Bierman, A. P. Colleraine, V. Nauenberg, Phys. Rev. 147, 922 (1966).

8. C. Lovelace, CERN 66/1257/5-TH. 705 (unpublished).

9. W. G. Holladay, Phys. Rev. 139B, 1348 (1965).

10. We take X=350 MeV, the fitted result obtained by S. L. Glashow and A. H. Rosenfeld, Phys. Rev. Letters 10, 192 (1963).

11. J. E. Rush and W. G. Holladay, Phys. Rev. 148, 1444 (1966).

12. R. D. Tripp, D. W. G. Leith, A. Minten, R. Armenteros, M. Ferro-Luzzi, R. Levi-Setti, H. Filthuth, V. Hepp, E. Kluge, H. Schneider, P. Barloutaud, P. Granet, J. Meyer, and J. P. Porte, UCRL-17385 Rev. (to be published).

13. G. F. Chew and F. A. Low, Phys. Rev. 113, 1640 (1959)
E. Ferrari, Phys Rev. 120, 988 (1960).
F. Salzman and G. Salzman, Phys. Rev. 121, 1541 (1961)
T. Yao, Phys. Rev. 125, 1048 (1962).

14. J. D. Jackson and H. Pilkuhn, Nuovo Cimento 33, 906 (1964)
J. D. Jackson and J. T. Donahue, Phys. Rev. 139B, 428 (1965).

15. The meson exchange calculations use data from the following references for associated production and $K^+p$ elastic scattering.
$K^+$; elastic scattering:
S. Goldhaber, W. Chinowsky, G. Goldhaber, Y. Lee, T. O'Halloran, T. F. Stubbs, G. M. Pjerrow, D. H. Stork, H. K. Ticho, Phys. Rev. Letters 9, 135 (1962)
T. F. Stubbs, H. Bradner, W. Chinowsky, G. Goldhaber, S. Goldhaber, W. Slater, D. M. Stork, H. K. Ticho, Phys. Rev. Letters 7, 188 (1961)
C. Wohl, private communication

A. Bettini, M. Cresti, S. Limentani, L. Peruzzo, R. Santangelo, D. Locke, D. J. Crennel, W. T. Davies, P. B. Jones, Phys. Letters 16, 83 (1965)

W. Chinowsky, G. Goldhaber, S. Goldhaber, T. O'Halloran, B. Schwarzchild, Phys. Rec. 139B, 1411 (1965)

J. Debaisieux, F. Grard, J. Heughebaert, L. Pape, R. Windmolders, R. George, Y. Goldschmidt-Clermont, V. P. Henri, D. W. G. Leith, G. R. Lynch, F. Muller, I.-M. Perreau, G. Otter, P. Sällström, Nuovo Cimento 43A, 142 (1966)

W. De Baere, J. Debaisieux, P. Dufour, F. Grard, J. Heughebaert, L. Pape, P. Peeters, F. Verbeure, R. Windmolders, R. George, Y. Goldschmidt-Clermont, V. P. Henri, B. Jongejans, D. W. G. Leith, A. Moisseev, F. Muller, J.-M. Perreau, V. Yarba, Nuovo Cimento 45A, 885 (1966).

$\pi^- p \rightarrow \Sigma^+ K^+$:

The data up to 1760 MeV/c is summarized by Holladay (Ref. 11).

D. Berley and N. Gelfand, Phys. Rev. 139, B1097 (1965).

D. R. O. Morrison, CERN/TCL Physics 66-20 (unpublished).

$\pi^- p \rightarrow \Lambda K^+$:

L. Bertanza, P. L. Connolly, B. B. Culwick, F. R. Eisler, T. Morris, R. Palmer, A. Prodell, N. P. Samios, Phys. Rev. Letters 8, 332 (1962).

Joseph Keren, Phys. Rev. 133, B457 (1964).

J. A. Anderson (Ph.D. Thesis) UCRL-10838 (unpublished).

F. Eisler, R. Plano, A. Prodell, N. Samios, M. Schwartz, J. Steinberger, P. Bassi, V. Borelli, G. Puppi, G. Tanaka, P. Woloscjek, V. Zobolli,

M. Conversi, P. Franzini, I. Mannelli, R. Santangelo, V. Silvestrini, Phys. Rev. 108, 1353 (1957).

O. I. Dahl, L. M. Hardy, R. I. Hess, J. Kirz, D. H. Miller, J. A. Schwartz, UCRL-17217 (submitted to the Physical Review).

The values for hyperon-nucleon-kaon coupling constants were communicated to us by J. K. Kim (to be published).

Table I. Event totals and cross sections for pp three-body reaction containing a K-meson at 6 BeV/c.

| Channel | Observed Number | Corrected Number | Cross section (μb) |
|---|---|---|---|
| $\Lambda pK^+$ | 916 | 1037 | $54.2 {}^{+3}_{-5}$ |
| $\Sigma^o pK^+$ | 254 | 285 | $17.0 {}^{+4}_{-2}$ |
| $\Sigma^+ pK^o$ | | | $26.0 \pm 4$ |
| $\Sigma^+ \to \pi^+(n)$ | 87 | 113[b] | |
| $\Sigma^+ \to p(\pi^o)$ | 45 | 56[b] | |
| $\Sigma^+ p(K^o)$[a] | | | $29 \pm 5$ |
| $\Sigma^+ \to \pi^+(n)$ | 84 | 126 | |
| $\Sigma^+ \to p(\pi^o)$ | 33 | | |
| $\Sigma^+ K^+(n)$ | | | $57 \pm 7$ |
| $\Sigma^+ \to \pi^+(n)$ | 255 | 395 | |
| $\Sigma^+ \to p(\pi^o)$ | 72 | | |

(a) Only half of the film was analysed for the two prong with decay topology.

(b) This number does not contain a correction for small angle $\Sigma^+$ decays.

Table II. Pion-nucleon resonances between 1600 and 2000 MeV/$c^2$.[a]

| $N^*$ | Resonant State | $M^o$(MeV) | $\Gamma_{elastic}$ (MeV) | $\Gamma_{inelastic}$ (MeV) |
|---|---|---|---|---|
| T=3/2 | $F_{7/2}$ | 1920 | 100 | 100 |
| T=1/2 | $S_{1/2}$ | 1700 | 216 | 24 |
| | $D_{5/2}$ | 1670 | 56 | 84 |
| | $F_{5/2}$ | 1688 | 72 | 38 |

(a) Values are quoted from UCRL-8030 (rev) Jan. 31, 1967.

## FIGURE CAPTIONS

Fig. 1. Schematic of experimental arrangement.

Fig. 2 Distributions of the cosine of the angle the final state proton makes with the beam in the overall center of mass, solid line: only unambiguously identified examples of the reaction $pp \rightarrow \Lambda pK^+$, dotted line: events ambiguous between hypotheses $pp \rightarrow \Lambda pK^+$, $pp \rightarrow \Sigma^o pK^+$.

Fig. 3 Distribution of the cosine of the proton center of mass angle for unambiguously identified examples of the reaction $pp \rightarrow \Sigma^o pK^+$.

Fig. 4. Dalitz plot for reaction $pp \rightarrow \Lambda pK^+$.

Fig. 5. Dalitz plot for reaction $pp \rightarrow \Sigma^o pK^+$.

Fig. 6. Dalitz plot for reaction $pp \rightarrow \Sigma^+ pK^o$.

Fig. 7. Dalitz plot for reaction $pp \rightarrow \Sigma^+ nK^+$.

Fig. 8. Mass distributions in the channel $\Lambda pK^+$, (a) $M(\Lambda K^+)$, (b) $M(\Lambda p)$, (c) $M(K^+p)$. The solid curves are phase space distributions while the dashed curves represent the effect of reflections, as discussed in the text.

Fig. 9. Mass distributions in the channel $\Sigma^o pK^+$, (a) $M(\Sigma^o K^+)$, (b) $M(\Sigma^o p)$. The curves are phase space distributions.

Fig. 10. Mass distributions in the channel $\Sigma^+ pK^o$, (a) $M(\Sigma^+ K^o)$, (b) $M(\Sigma^+ p)$. The curves are phase space distributions.

Fig. 11. Mass distributions in the channel $\Sigma^+ nK^+$, (a) $M(\Sigma^+ K^+)$, (b) $M(\Sigma^+ p)$. The curves are phase space distributions.

Fig. 12 The $\Lambda$-p mass distribution for the channel $\Lambda pK^+$ shown as a function of momentum transfer to the proton. The curves are phase space distributions.

Fig. 13. Decay angular distribution of the $\Sigma^+K^+$ system produced in the channel $\Sigma^+K^+n$. The angle $\theta$ is between the $\Sigma^+$ and momentum transfer directions in the $\Sigma^+K^+$ rest system. The curves are predictions of pion exchange with a form factor.

Fig. 14. Decay angular distribution of the $\Lambda K^+$ system. The angle $\theta$ is between the $\Lambda$ and momentum transfer directions in the $\Lambda K^+$ rest system. The curves are predictions of pion exchange with a form factor.

Fig. 15. Scatter plot of $\Lambda K^+$ mass vs. momentum transfer for reaction $pp \rightarrow \Lambda K^+$.

Fig. 16. Scatter plot of $\Sigma^+K^+$ mass vs. momentum transfer for reaction $pp \rightarrow \Sigma^+nK^+$.

Fig. 17. The three single particle exchange diagrams applicable to the reactions $pp \rightarrow \Lambda pK^+$, $pp \rightarrow \Sigma^+K^+n$. (a) pion exchange, (b) kaon exchange, (c) baryon exchange.

Fig. 18. (a) Distribution of momentum transfer to the final state proton for reaction $pp \rightarrow \Lambda pK^+$. The smooth curve is the pion exchange prediction.

(b) Distribution in momentum transfer to the $\Lambda$. The smooth curve is the K exchange prediction. The theoretical curves are normalized to the experimental histograms.

Fig. 19. $\Lambda K^+$ mass distributions for the reaction $pp \rightarrow \Lambda pK^+$. The solid curve is the pion exchange prediction and the dashed curve that for K exchange. Both are normalized to the experimental histogram.

Fig. 20. $\Sigma^+K^+$ mass distribution for the reaction $pp \rightarrow \Sigma^+nK^+$. The solid curve is the pion exchange prediction and the dashed curve that for K exchange. Both are normalized to the experimental histogram.

Fig. 21. Lambda polarization for the reaction $pp \rightarrow \Lambda pK^+$ as a function of $\Lambda K^+$ mass. Polarizations for small momentum transfer events and pion exchange predictions are shown.

Fig. 22. Treiman-Yang distribution for the reaction $pp \rightarrow \Lambda pK^+$ as a function of momentum transfer. The smooth curves are predicted by pion exchange and are normalized to the experimental histograms.

Fig. 23. Treiman-Yang angle distribution for the reaction $pp \rightarrow \Sigma^+K^+n$ as a function of momentum transfer.

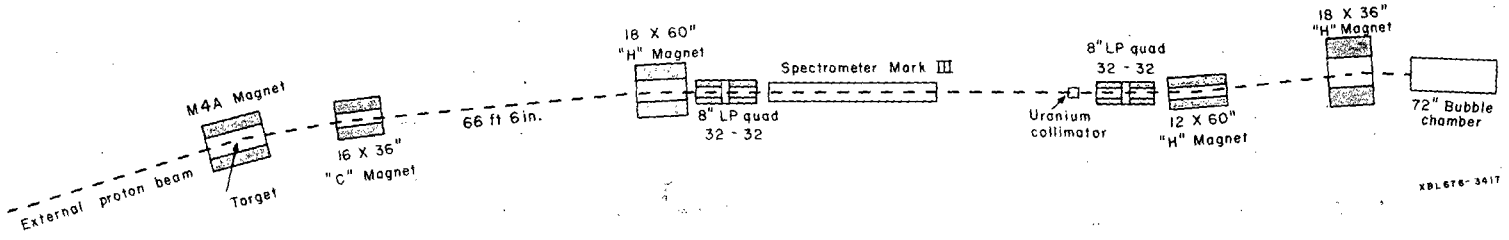
External proton beam
M4A Magnet
Target
16 X 36"
"C" Magnet
66 ft 6 in.
18 X 60"
"H" Magnet
8" LP quad
32 - 32
Spectrometer Mark III
Uranium
collimator
8" LP quad
32 - 32
12 X 60"
"H" Magnet
18 X 36"
"H" Magnet
72" Bubble
chamber
XBL 676-3417

Figure 1

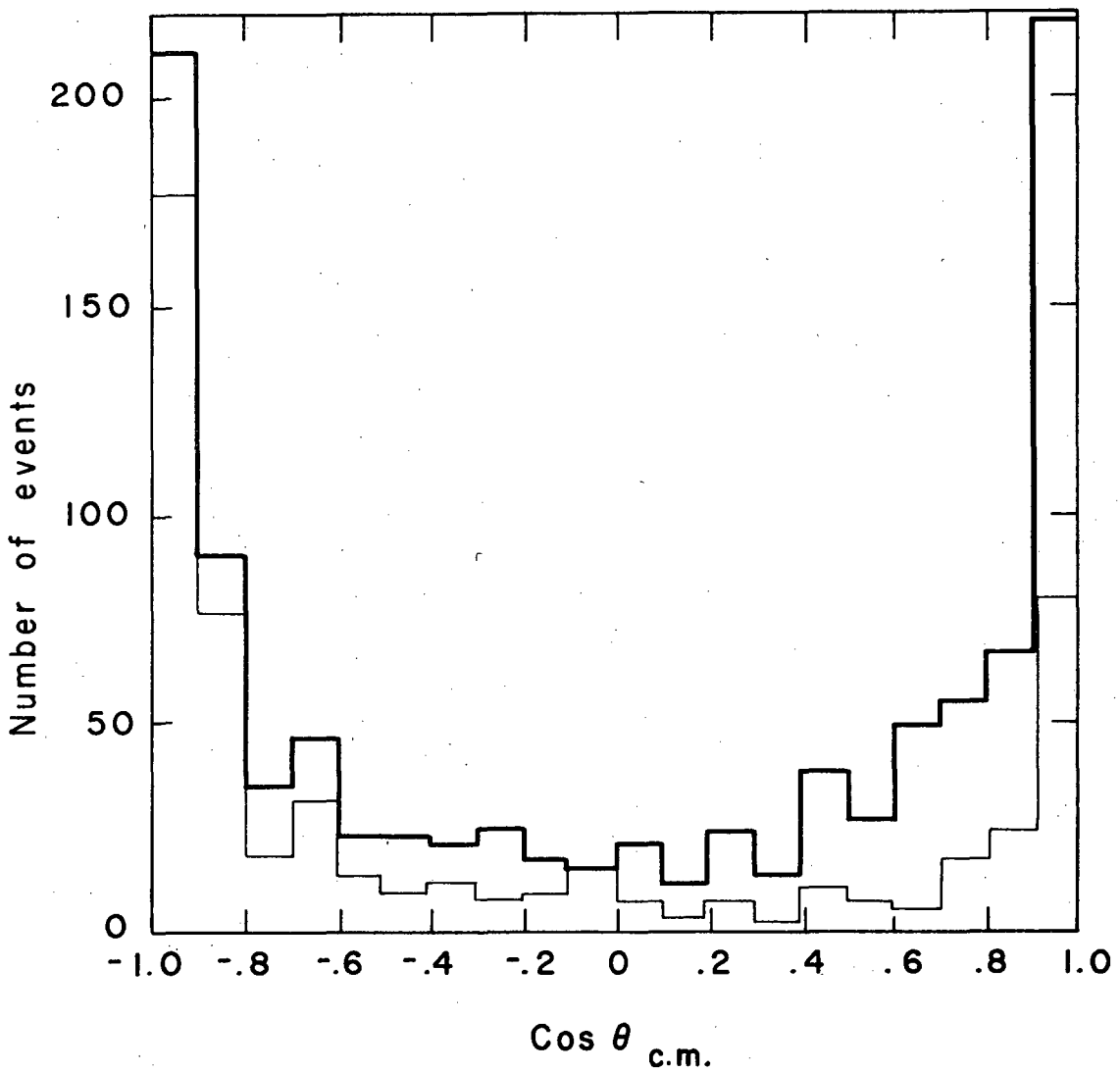


XBL 676-3405

Figure 2

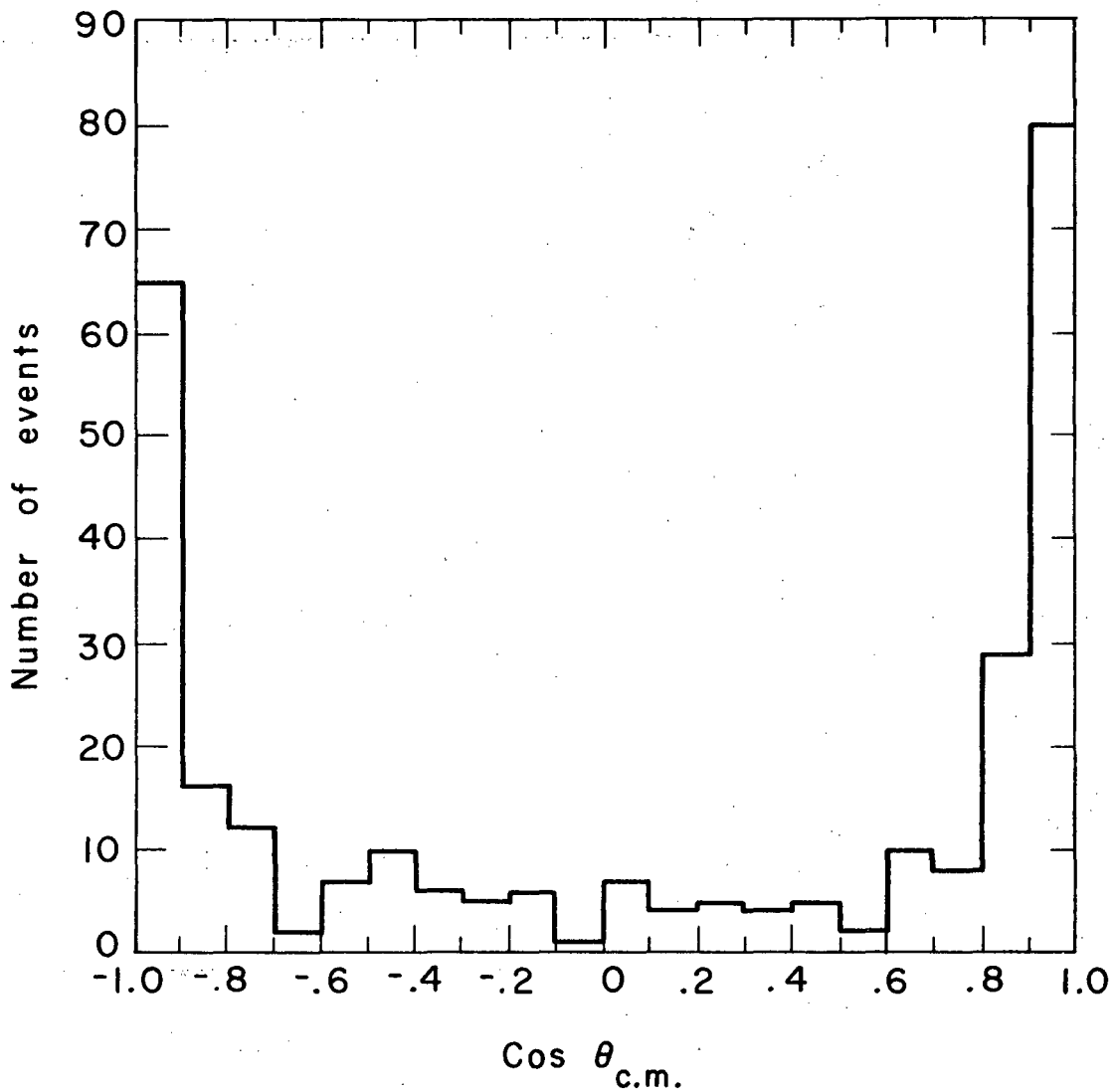


XBL 676-3406

Figure 3

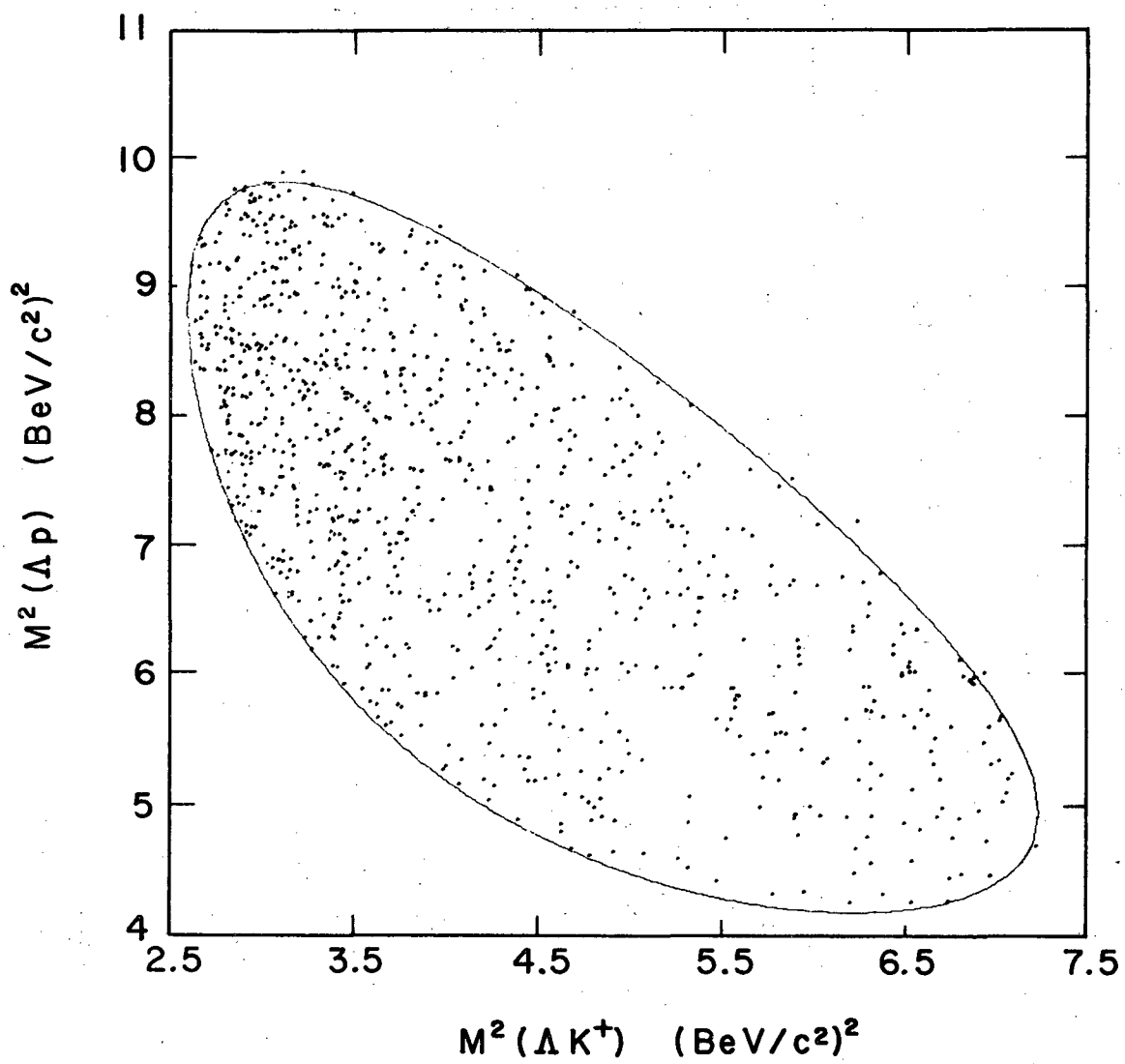


XBL676-3407

Figure 4

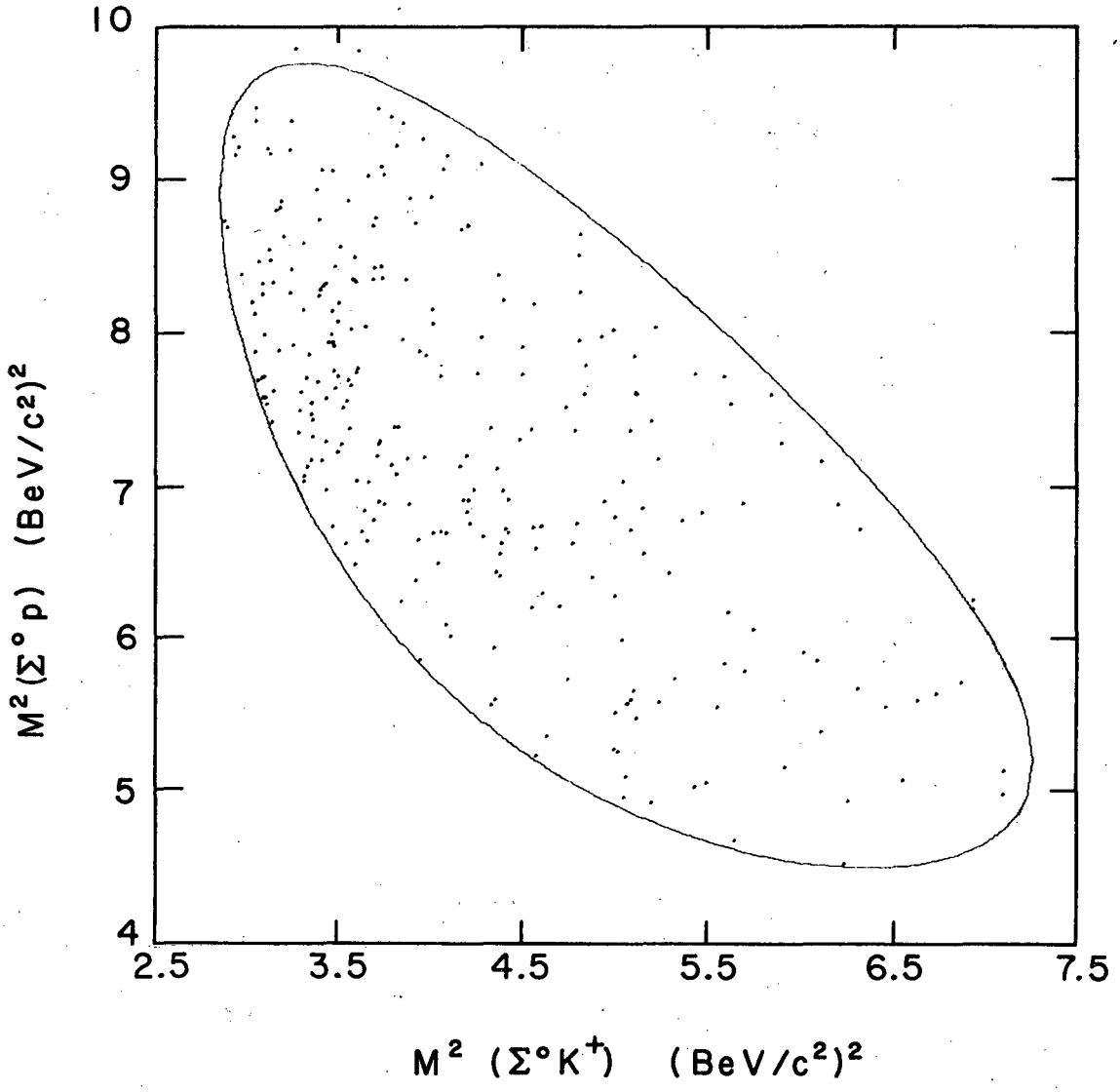


XBL676-3408

Figure 5

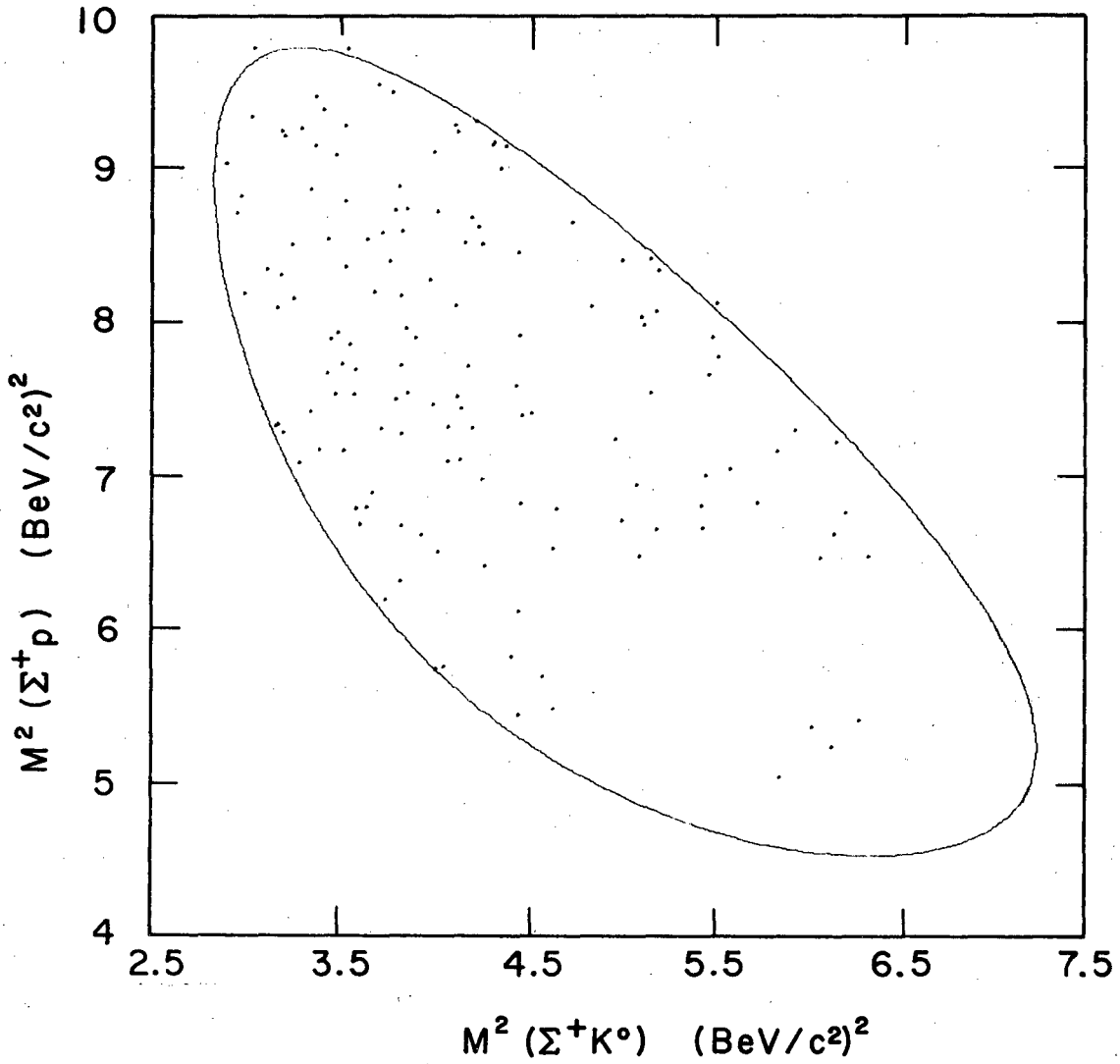


XBL 676-3409

Figure 6

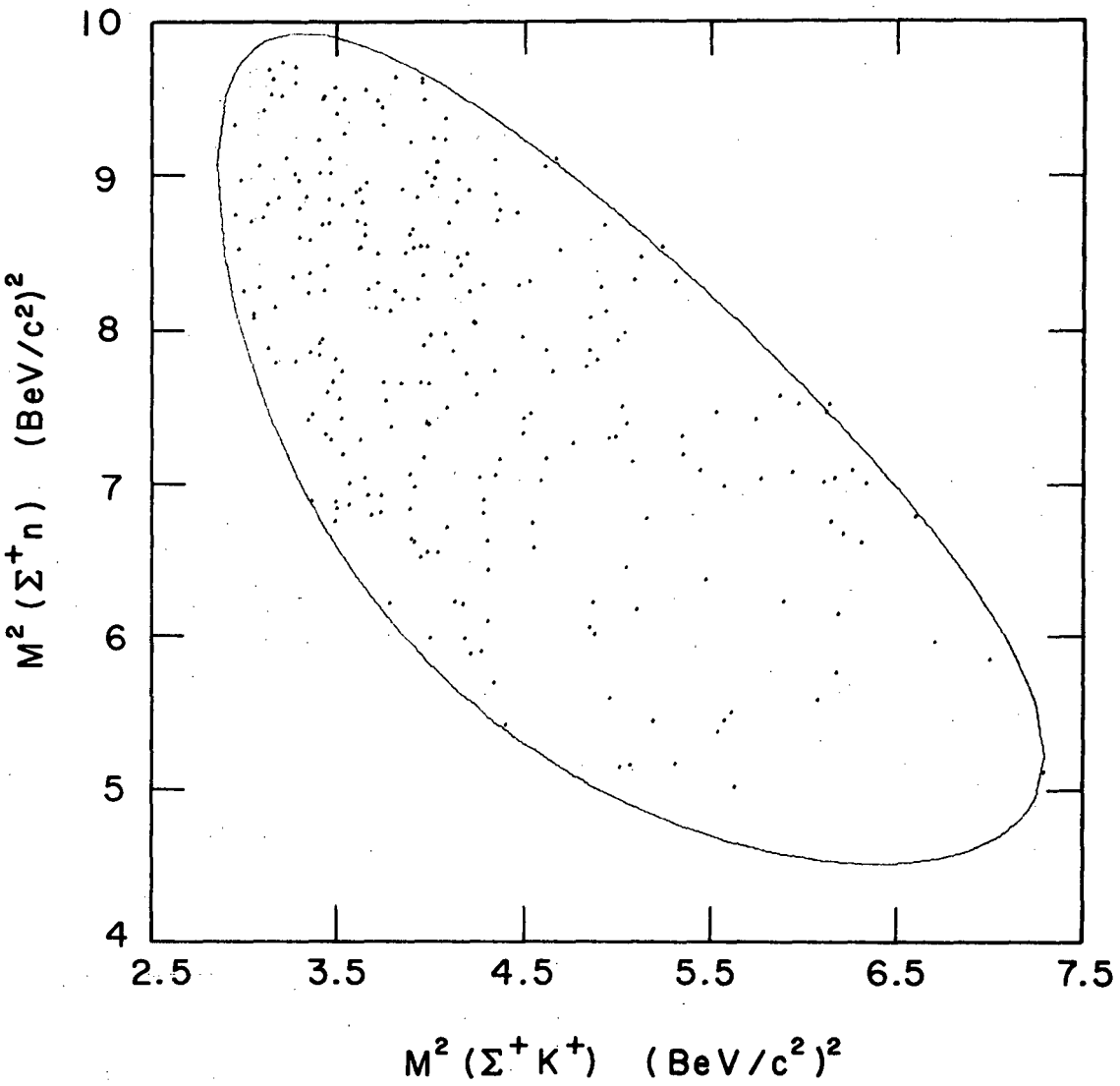


XBL676-3410

Figure 7

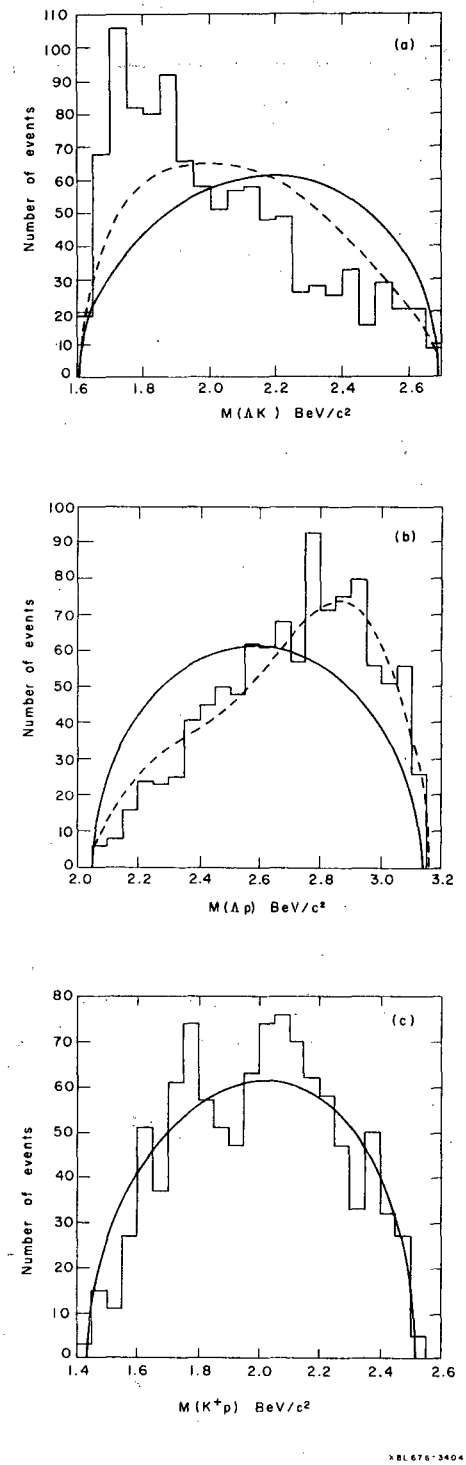
(a)
Number of events
M(ΛK) BeV/c²
(b)
Number of events
M(Λp) BeV/c²
(c)
Number of events
M(K⁺p) BeV/c²
XBL676-3404

Figure 8

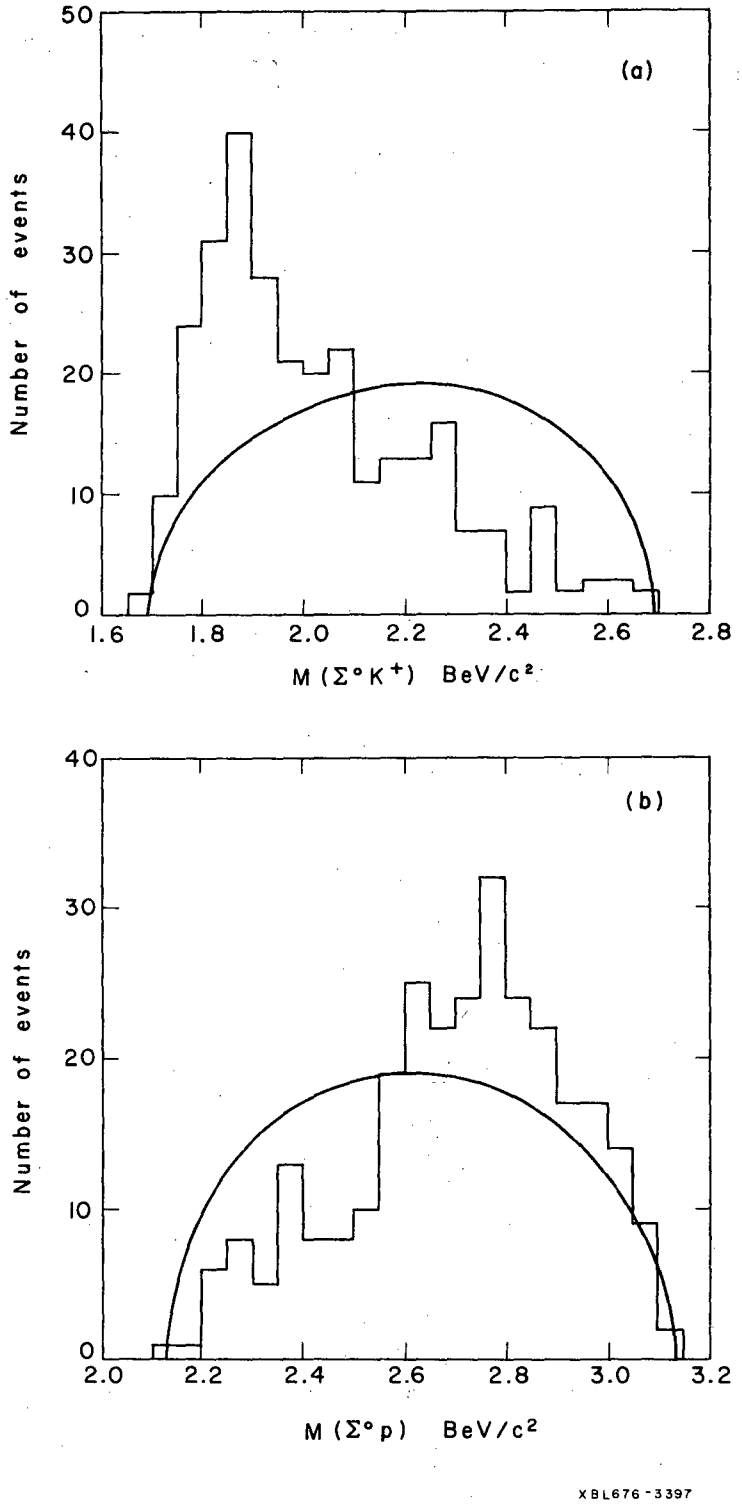
(a)
Number of events
50
40
30
20
10
0
1.6
1.8
2.0
2.2
2.4
2.6
2.8
M (Σ° K⁺) BeV/c²
(b)
Number of events
40
30
20
10
0
2.0
2.2
2.4
2.6
2.8
3.0
3.2
M (Σ° p) BeV/c²
XBL676-3397

Figure 9

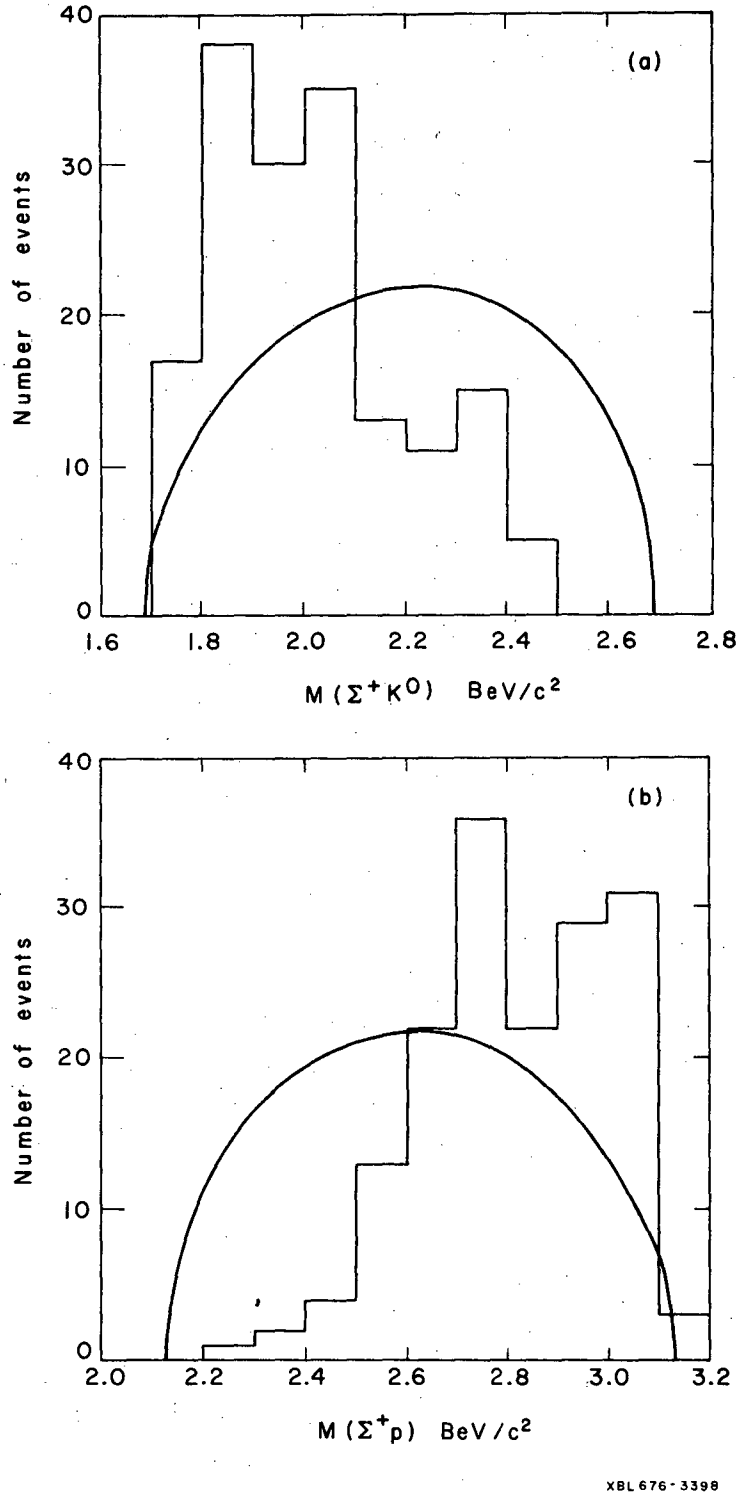
(a)
Number of events
40
30
20
10
0
1.6
1.8
2.0
2.2
2.4
2.6
2.8
M ($\Sigma^+ K^0$) BeV/c$^2$
(b)
Number of events
40
30
20
10
0
2.0
2.2
2.4
2.6
2.8
3.0
3.2
M ($\Sigma^+ p$) BeV/c$^2$
XBL 676-3398

Figure 10

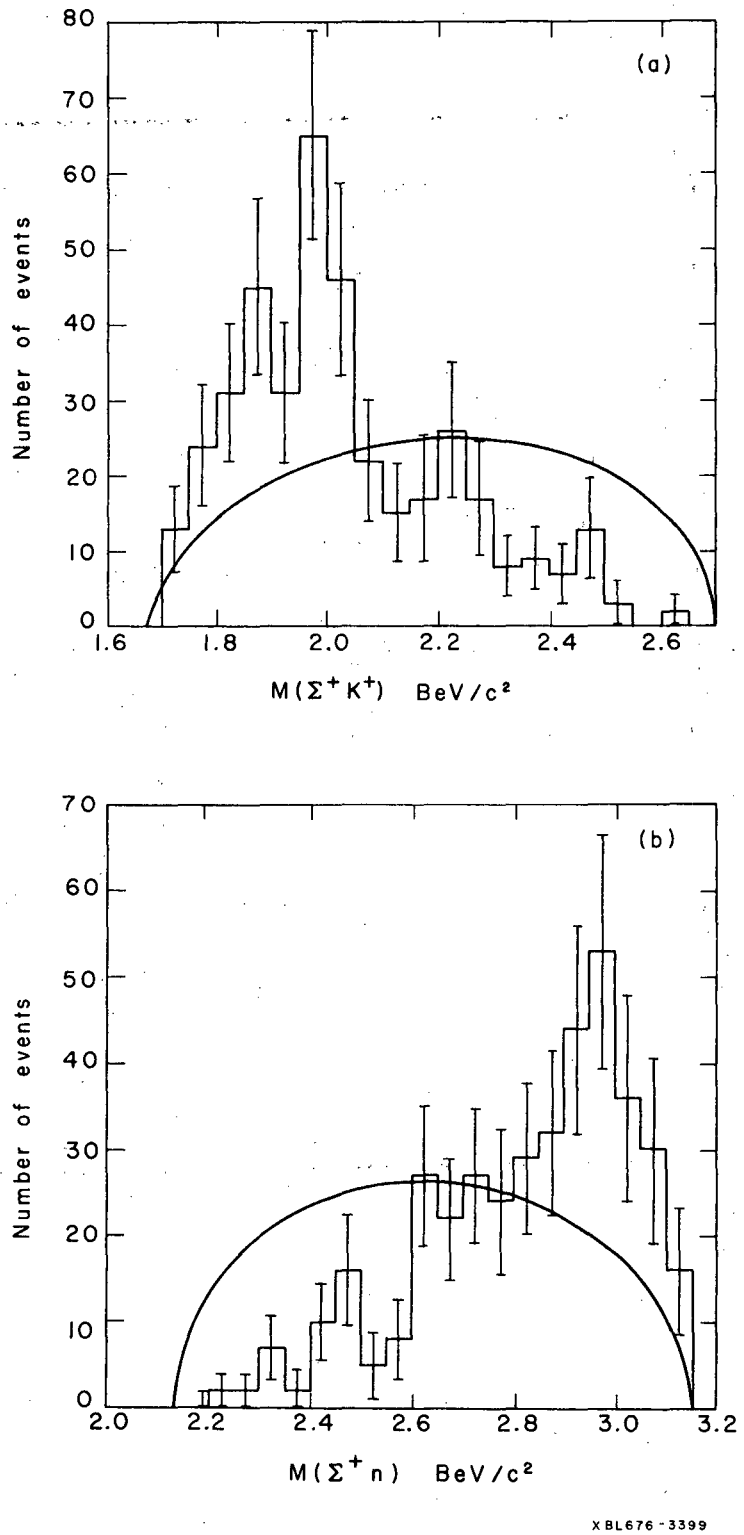
(a)
Number of events
M(Σ⁺K⁺) BeV/c²
(b)
Number of events
M(Σ⁺n) BeV/c²
XBL676-3399

Figure 11

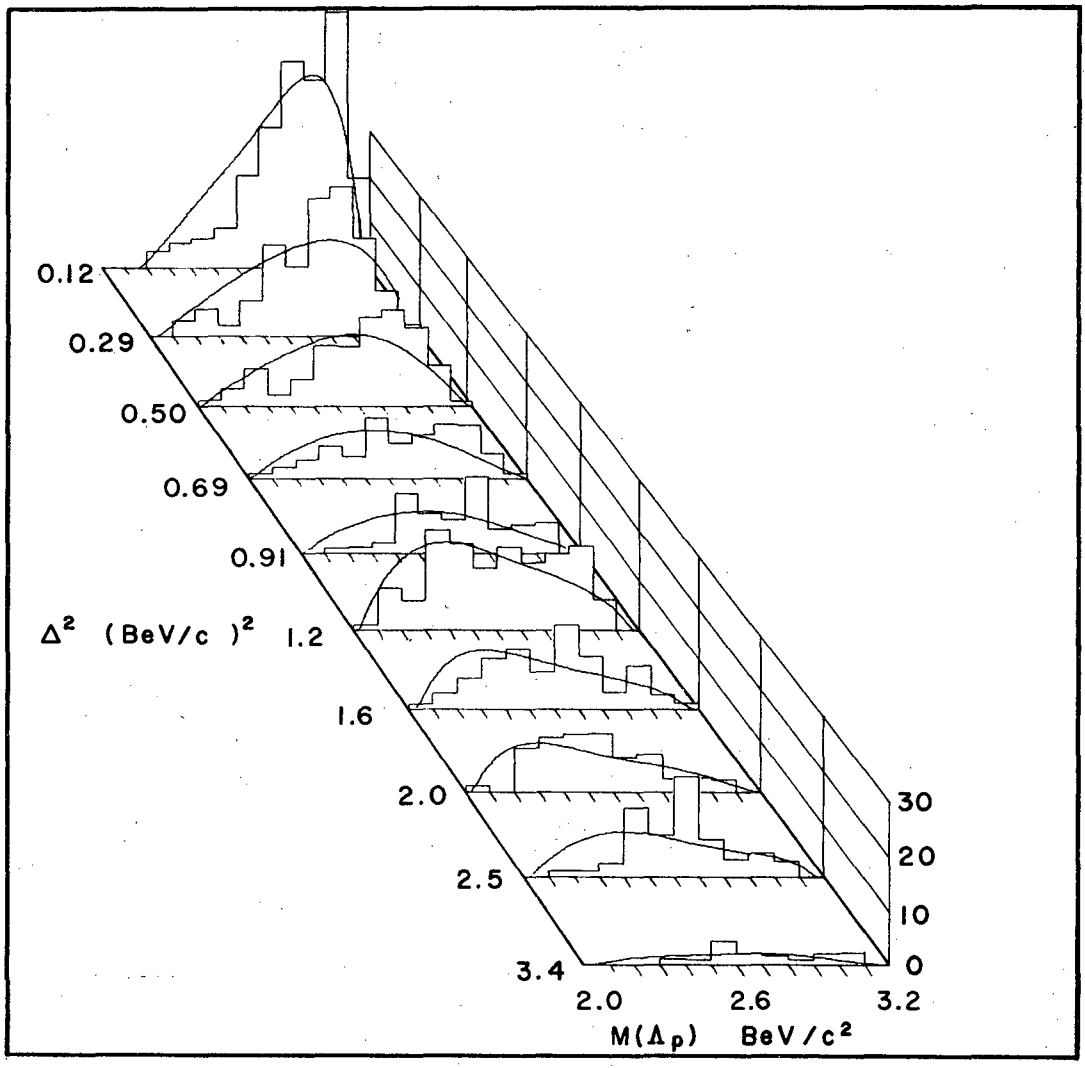


XBL676-3413

Figure 12

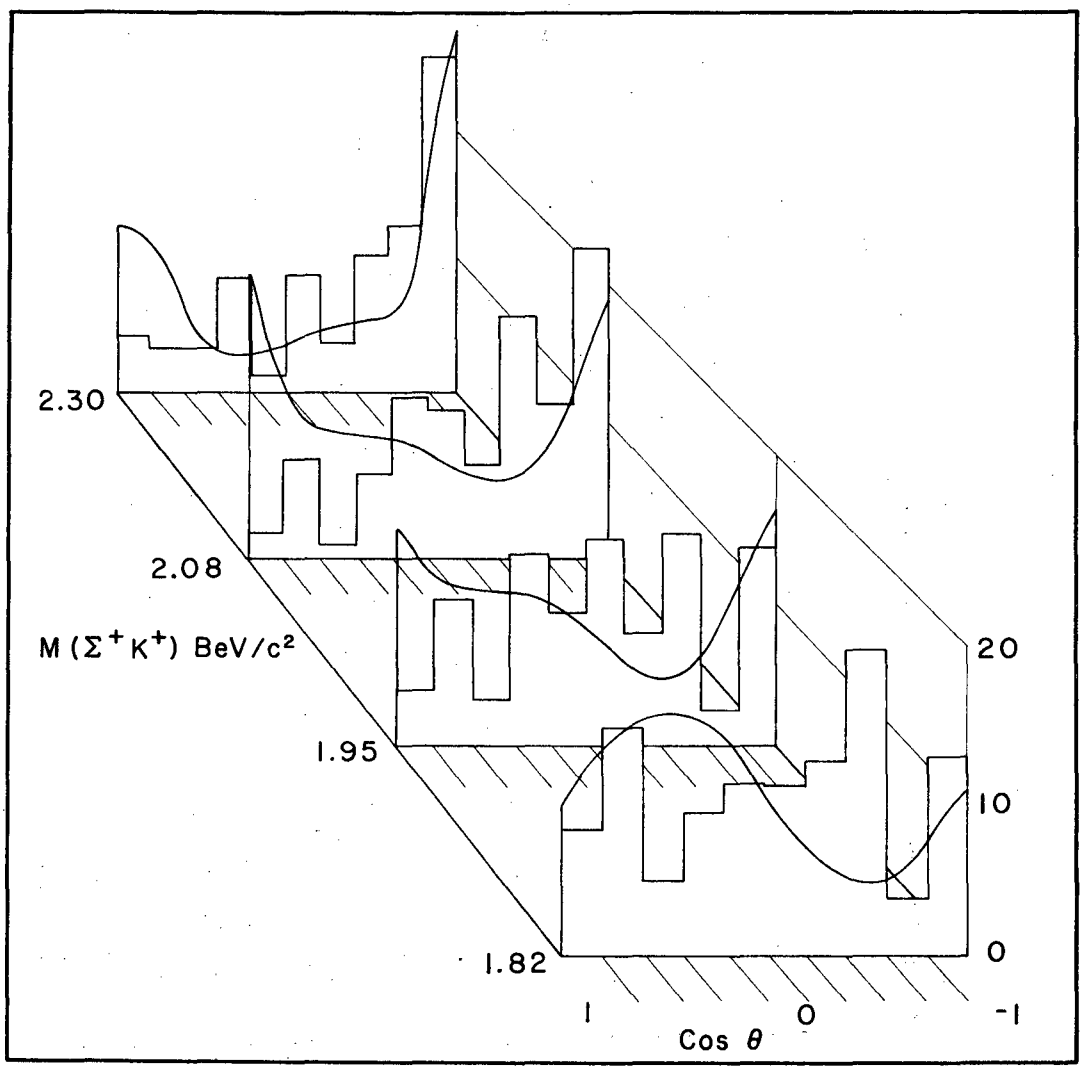


XBL676-3415

Figure 13

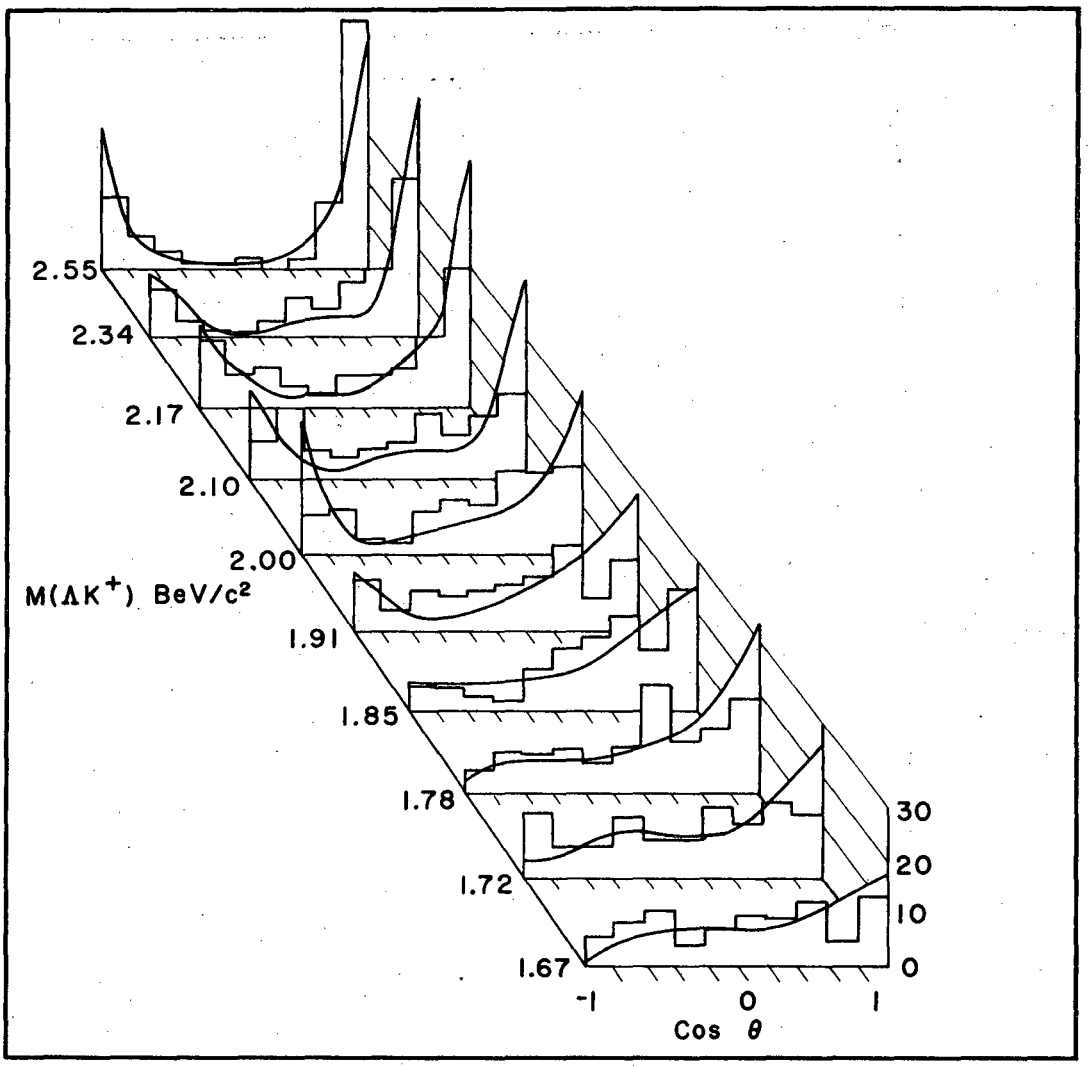


XBL676-3414

Figure 14

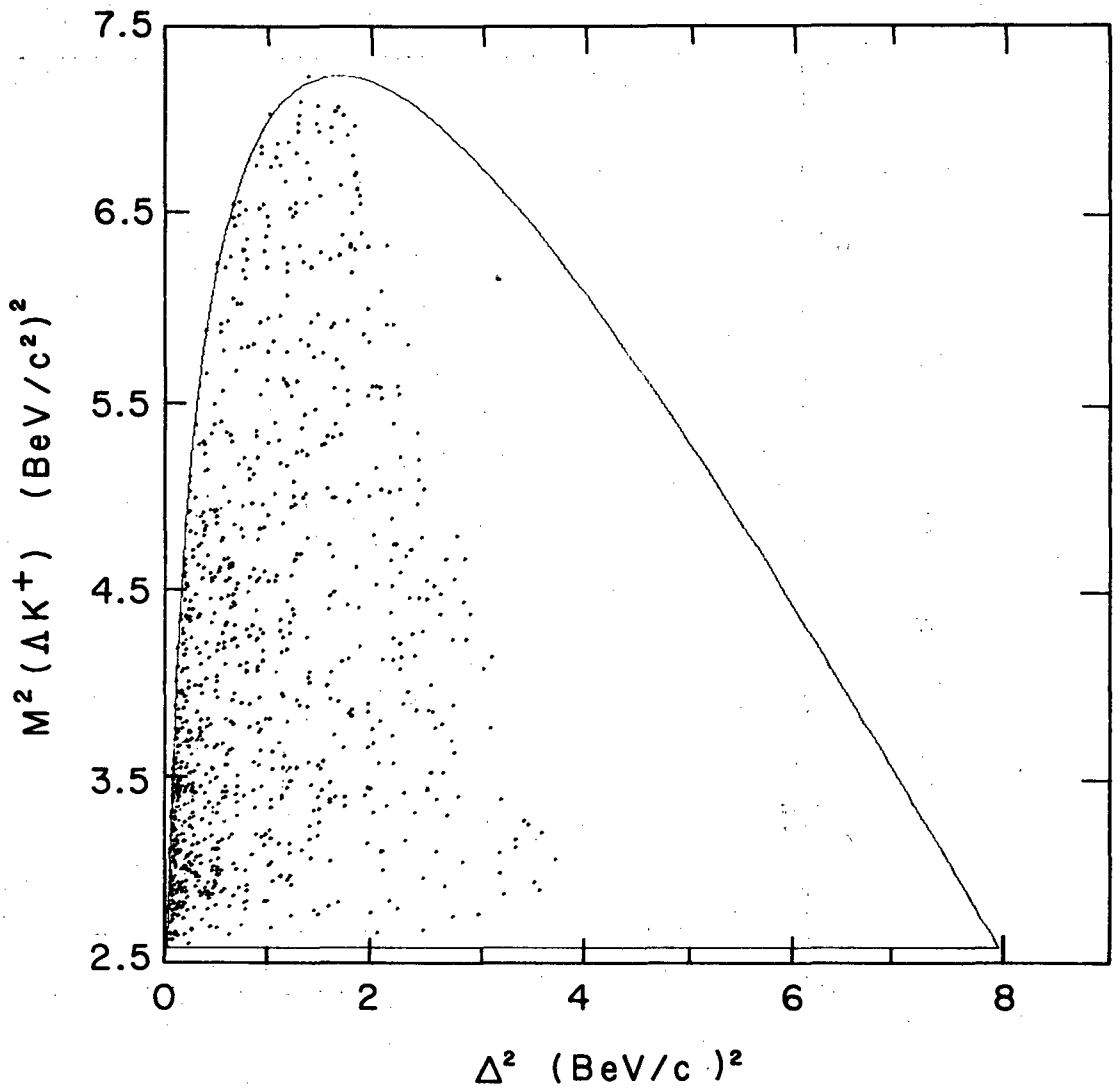


XBL 676-3400

Figure 15

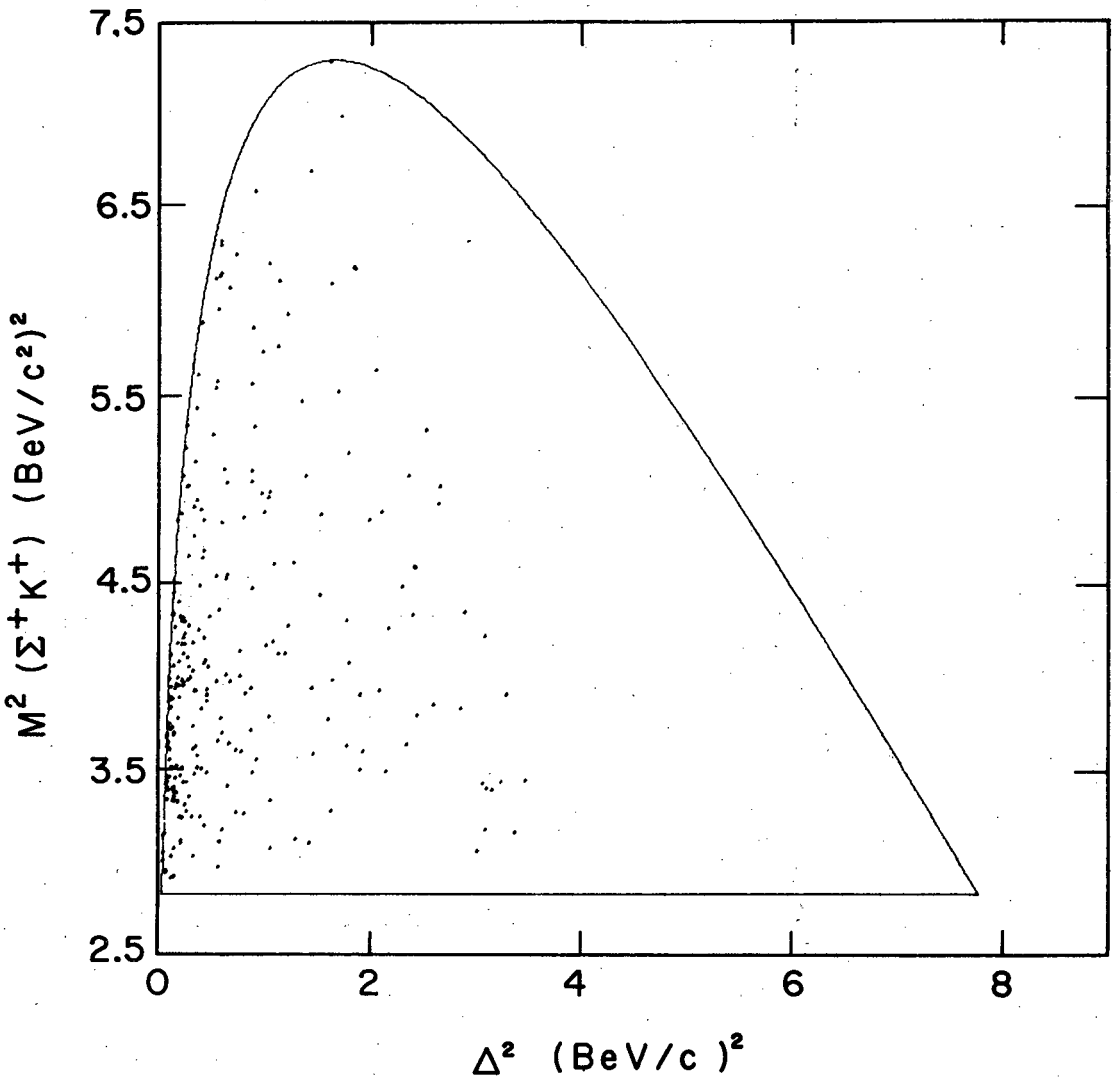


XBL676-3401

Figure 16

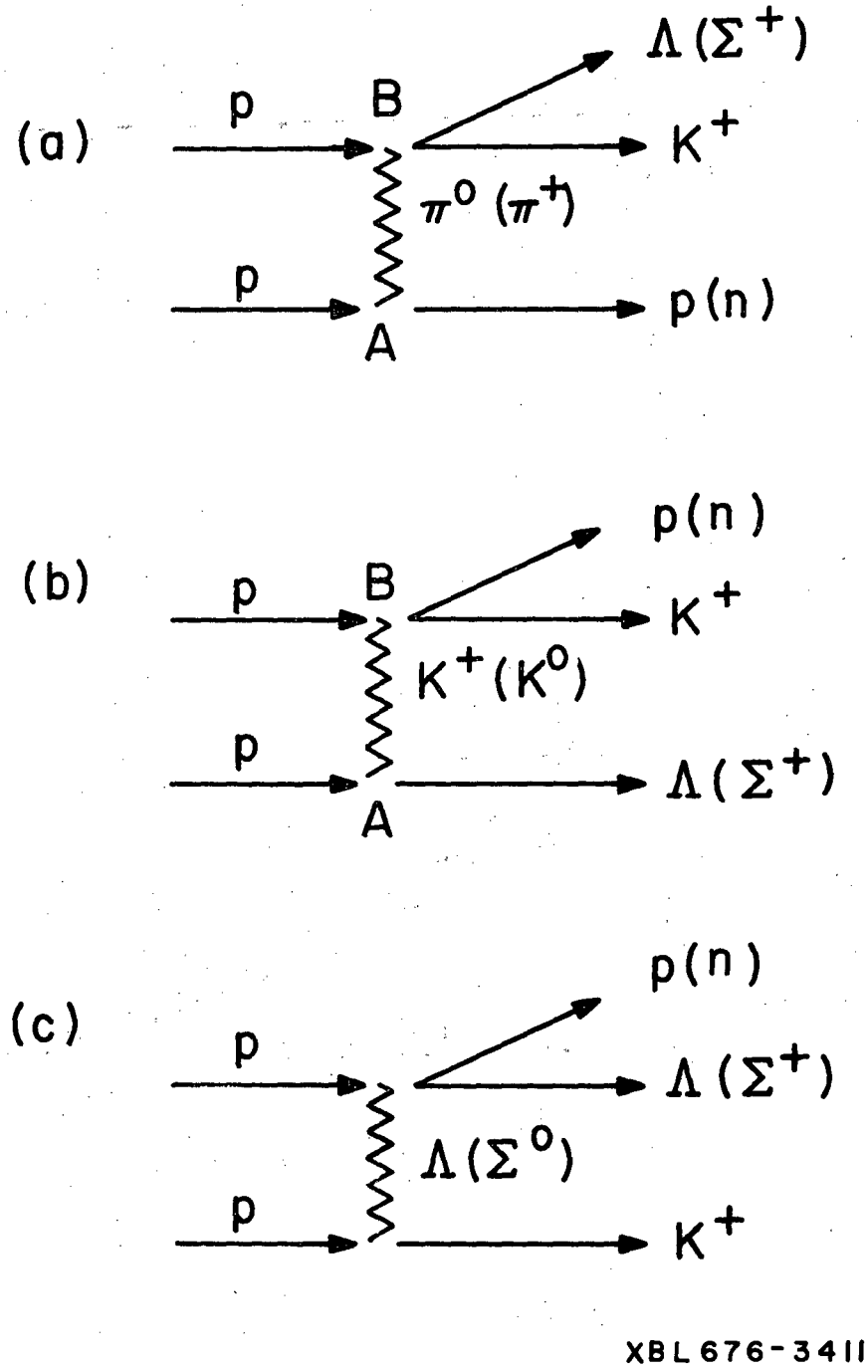


Figure 17

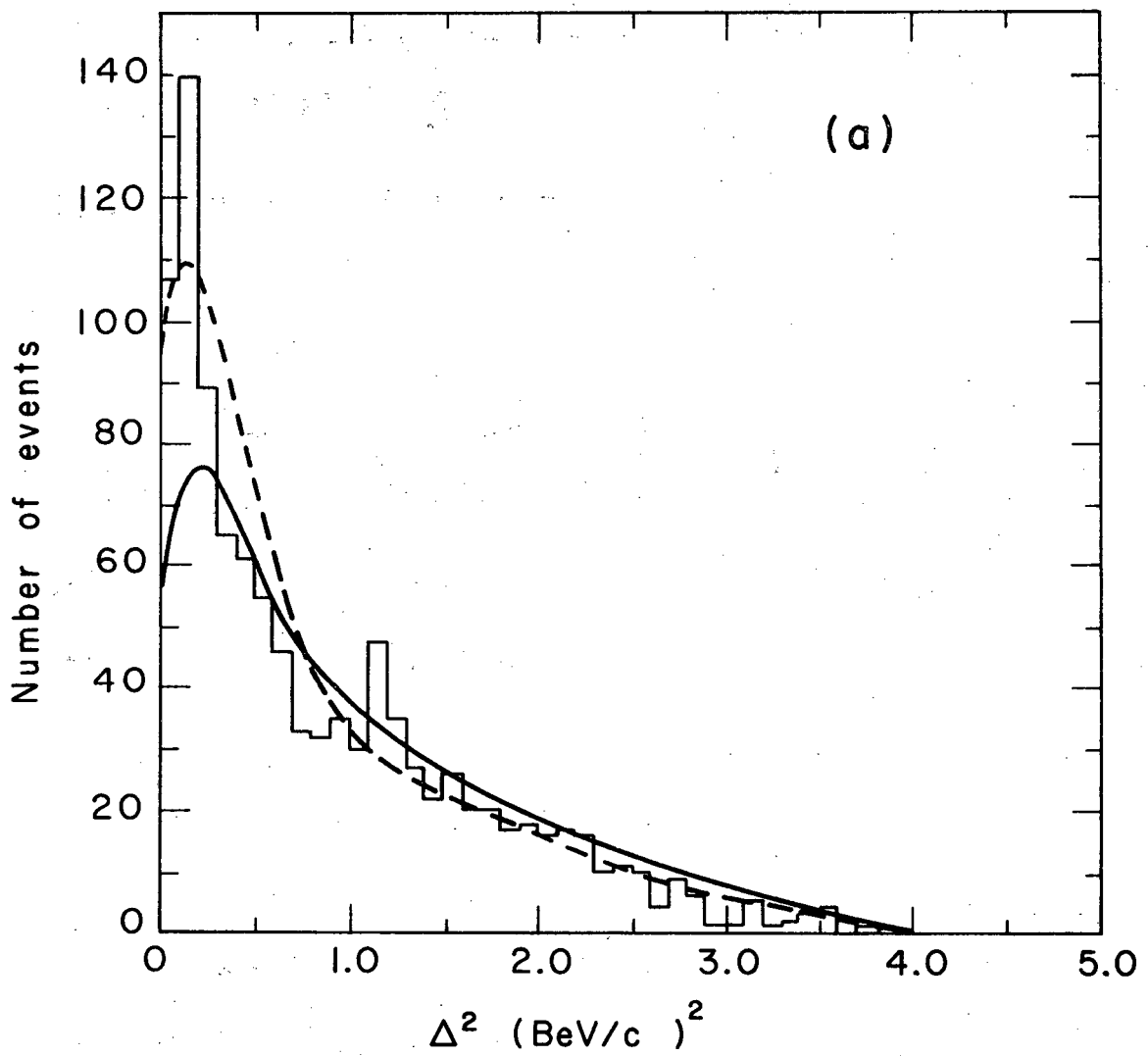


XBL676-3402

Figure 18a

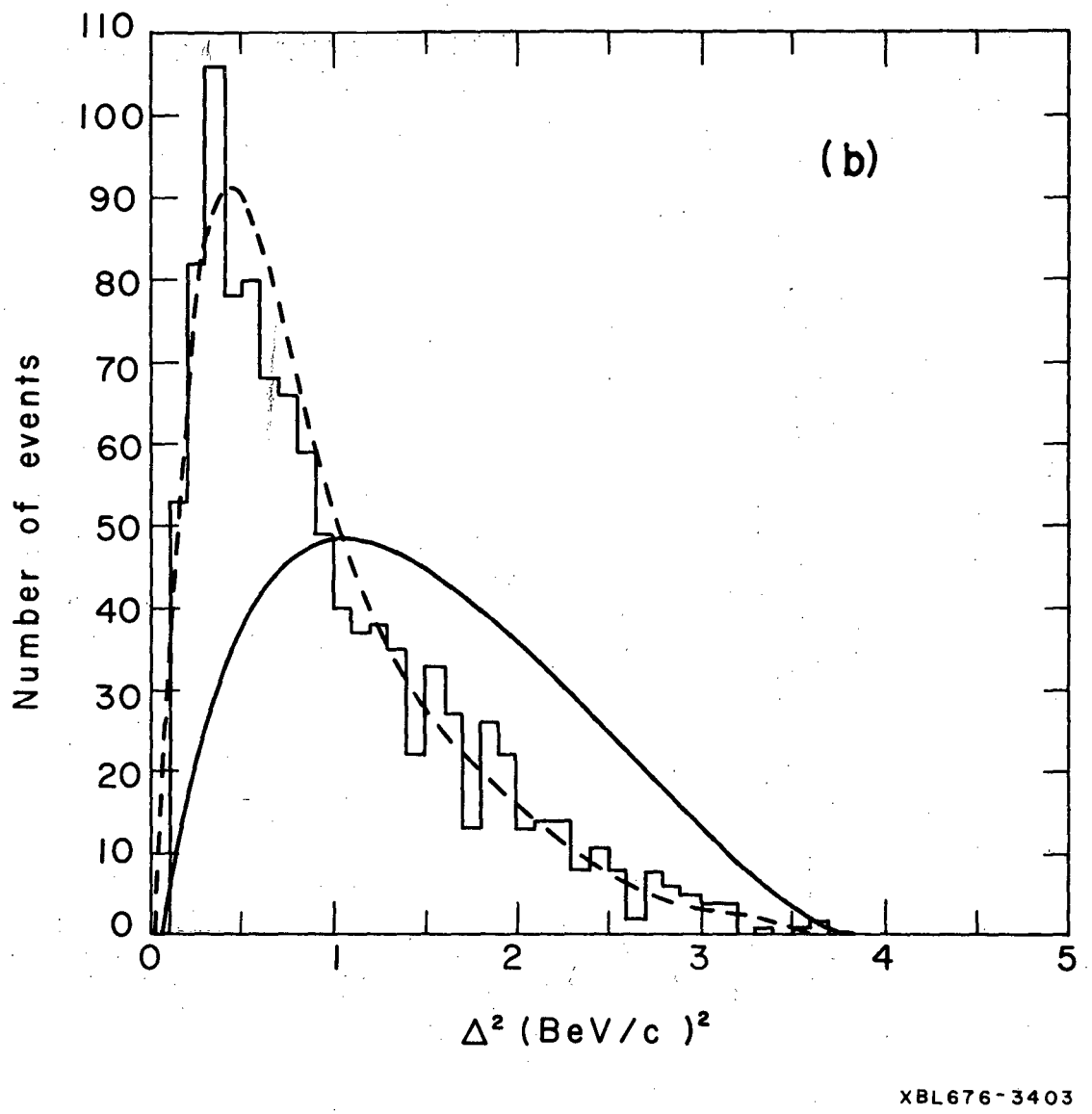
(b)
Number of events
110
100
90
80
70
60
50
40
30
20
10
0
0
1
2
3
4
5
Δ² (BeV/c )²
XBL676-3403

Figure 18b

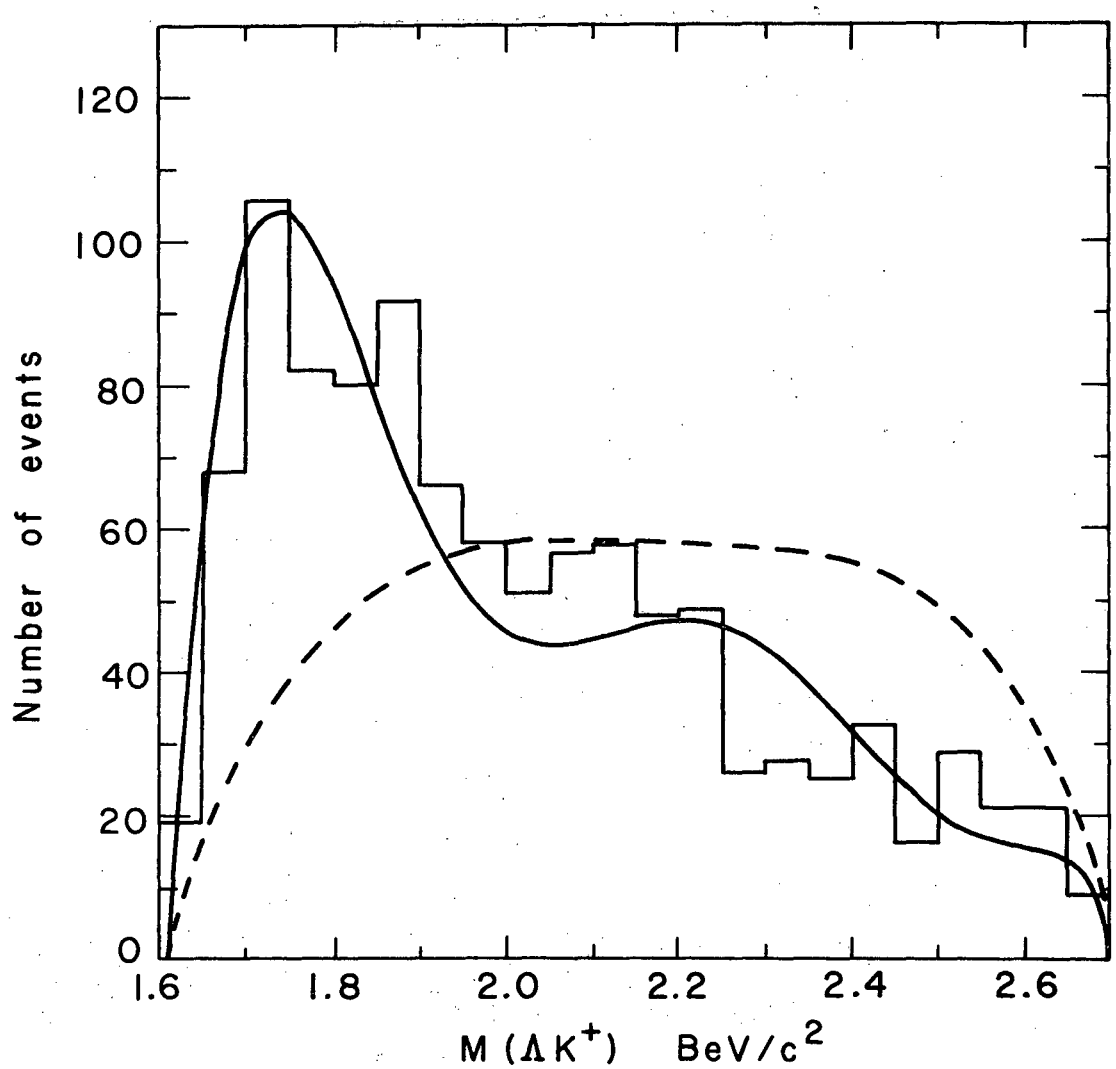


XBL676-3396

Figure 19

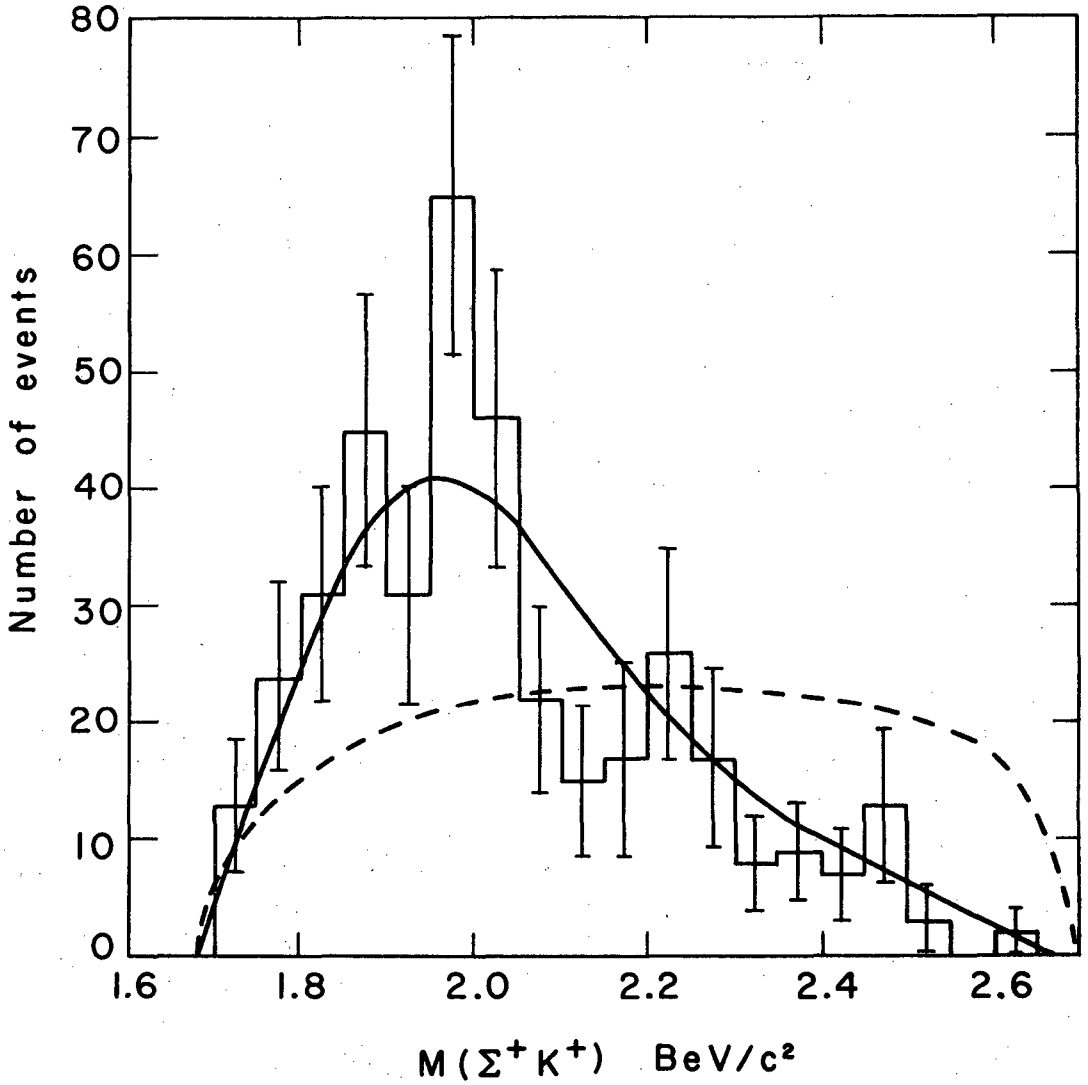


XBL676-3395

Figure 20

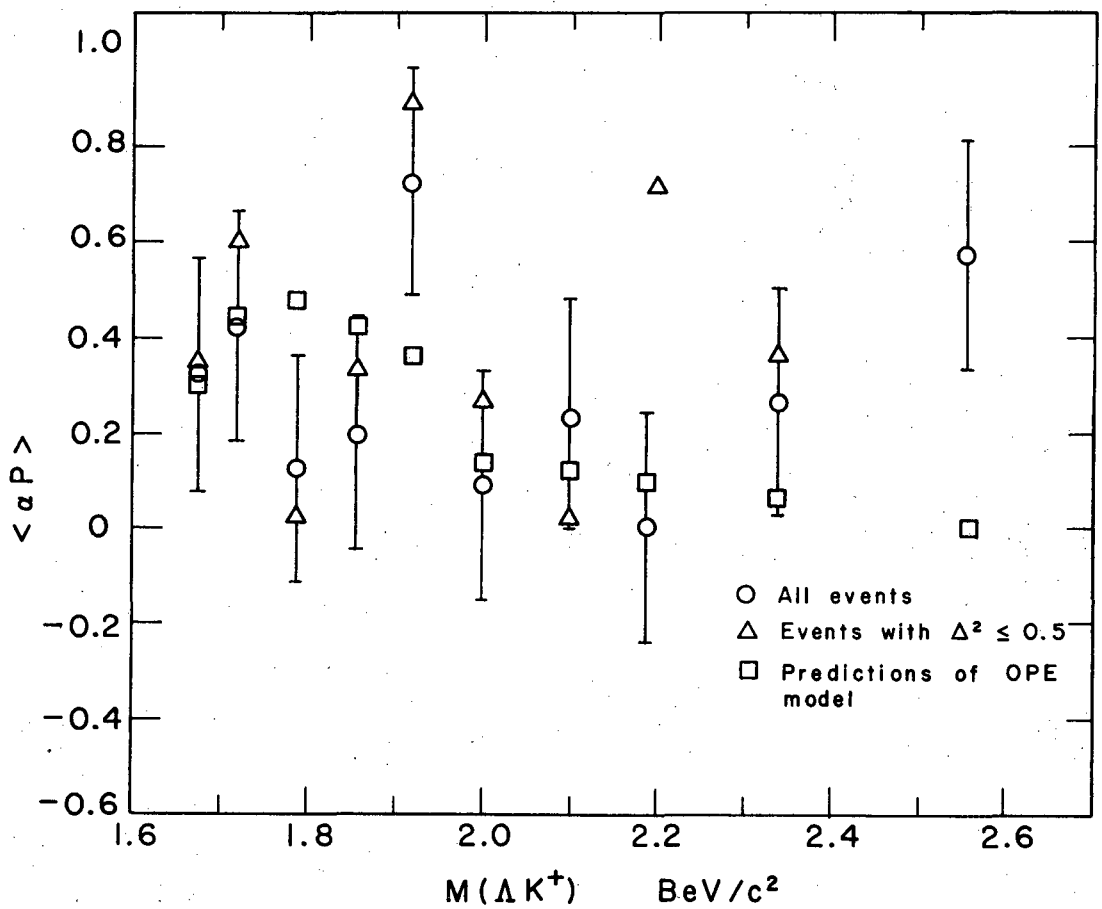


XBL677-3532

Figure 21

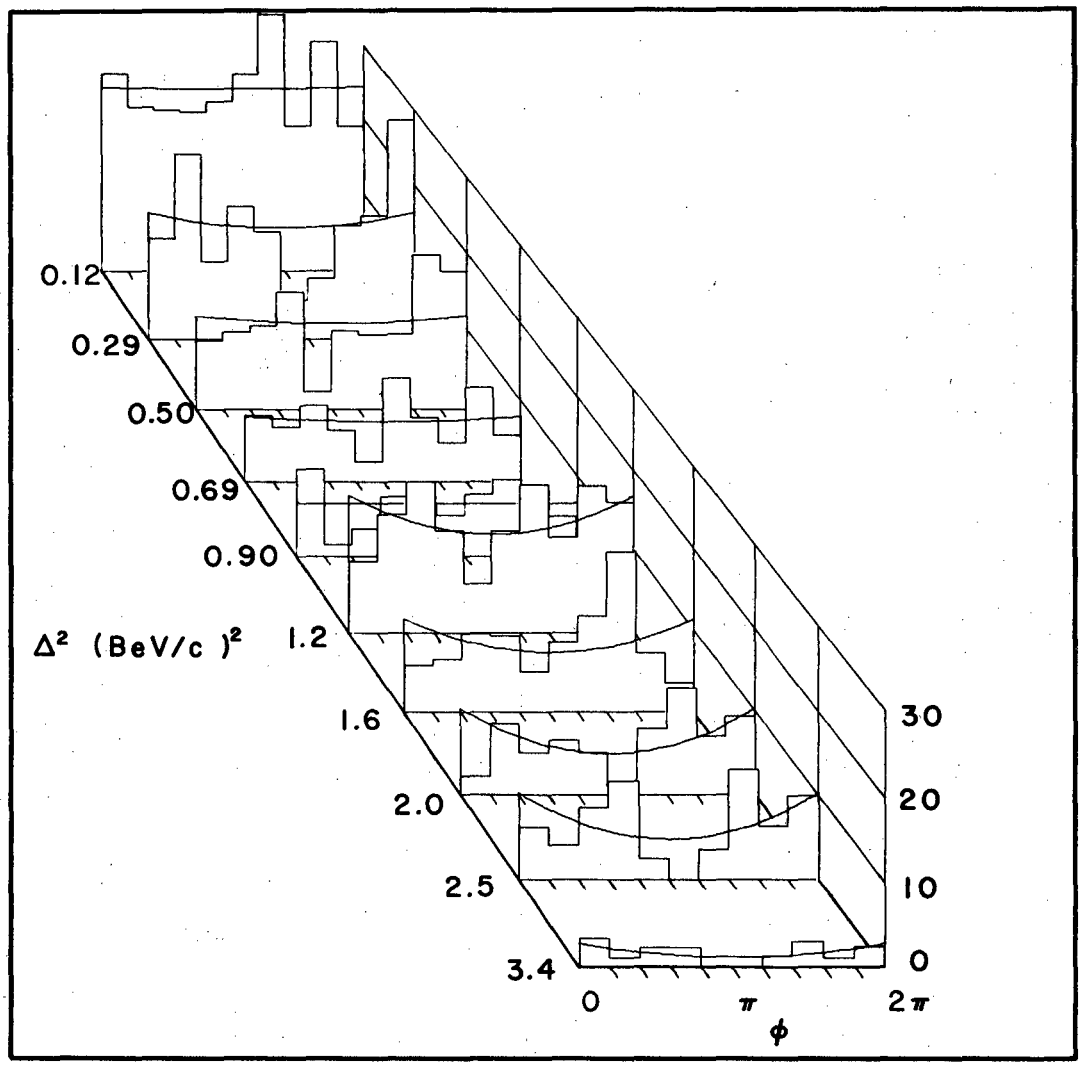


XBL676-3416

Figure 22

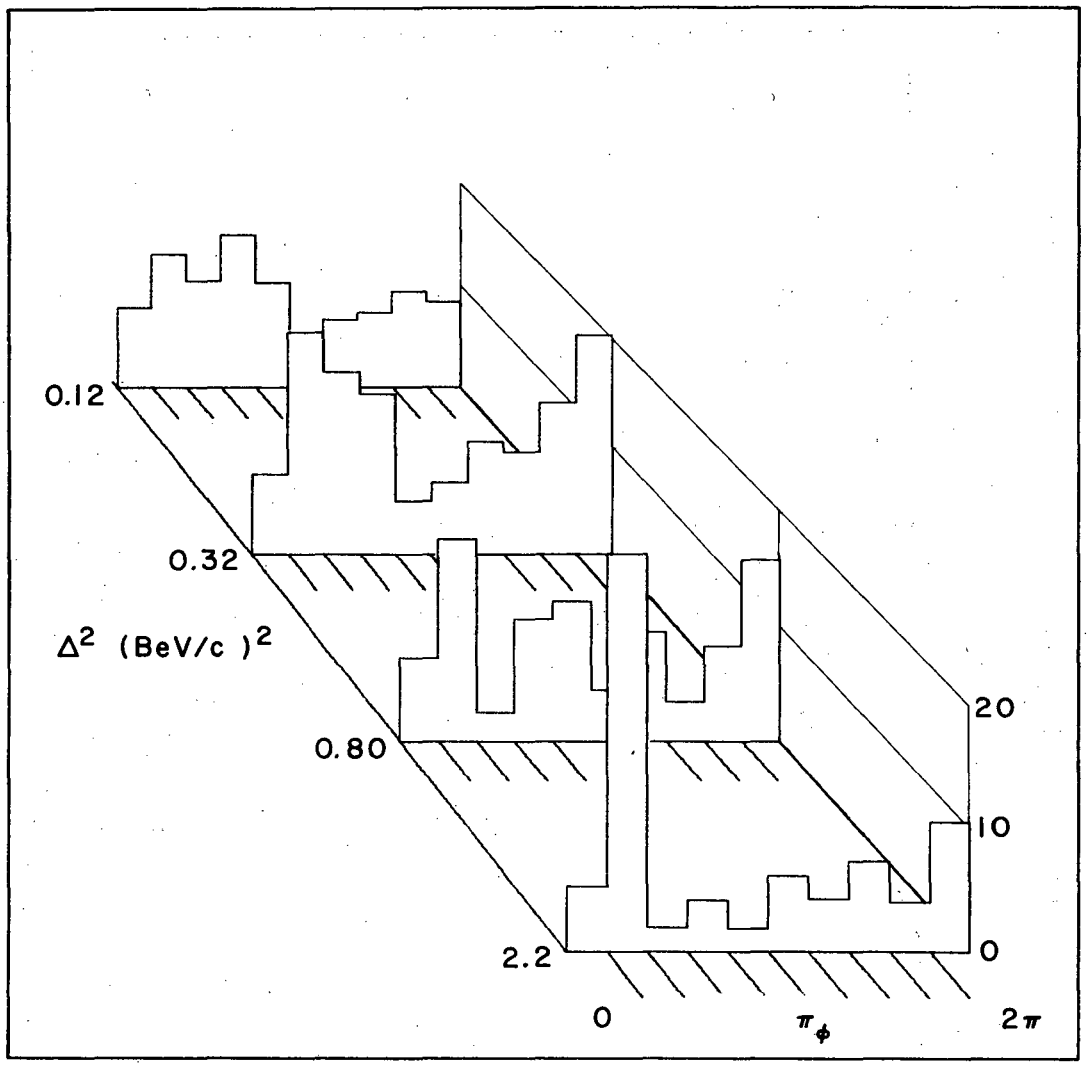


XBL676-3412

Figure 23

This report was prepared as an account of Government sponsored work. Neither the United States, nor the Commission, nor any person acting on behalf of the Commission:

A. Makes any warranty or representation, expressed or implied, with respect to the accuracy, completeness, or usefulness of the information contained in this report, or that the use of any information, apparatus, method, or process disclosed in this report may not infringe privately owned rights; or

B. Assumes any liabilities with respect to the use of, or for damages resulting from the use of any information, apparatus, method, or process disclosed in this report.

As used in the above, "person acting on behalf of the Commission" includes any employee or contractor of the Commission, or employee of such contractor, to the extent that such employee or contractor of the Commission, or employee of such contractor prepares, disseminates, or provides access to, any information pursuant to his employment or contract with the Commission, or his employment with such contractor.